SYNTHESIS OF TUNGSTEN CARBIDE NANOPARTICLES BY REFLUX REACTION

Thesis submitted in partial fulfilment of the requirement for
The award of the degree of

Master of Technology

In

MATERIALS SCIENCE AND ENGINEERING

Submitted by

RAJ KUMAR CHOPRA

Roll No - 60702015

Under the guidance of

Dr. O.P PANDEY

School of Physics & Materials Science

Thapar University, Patiala

Patiala - 147001

June-2009

CERTIFICATE

This is to certify that Mr. Raj Kumar Chopra, Roll No 60702015 has worked on this thesis report "**Synthesis of WC nanoparticles by reflux reaction**" as a partial fulfilment for award of the degree of **MASTER OF TECHNOLOGY** in **Material Science and Engineering**. I certify that the matter embodied in this report is one of the candidate's own record and not submitted to any other university in any part or full form for the award of such kind of degree.

23/6/09

(Dr. O. P Pandey)

Supervisor

School of Physics and Material Science

THAPAR UNIVERSITY

PATIALA.

Countersigned By

23/6/09

Dr. O. P Pandey

(Prof. and Head)

School of Physics and Material Science,

THAPAR UNIVERSITY, PATIALA

24/7/09

Dr. R. K Sharma

Dean of Academic Affairs

THAPAR UNIVERSITY,

PATIALA.

A KNOWLEDGEMENT

No matter how much enterprising and entrepreneurial one's thinking is, yet nobody can do everything all by himself without some help and guidance. It is inhumane if the concerned person assistance goes without appreciation and thanks. My first and foremost offering of thanks goes to the architect who shaped my dreams into reality, my guide and mentor **Dr. O.P Pandey**, Prof and Head, School of Physics and Material science, Thapar university, Patiala. Perseverance and positive approaches are some of the traits he imprinted on my personality. He steered me through his journey through his advice, positive attitude, stimulating discussion and consistent encouragement. His meticulous attention towards my proceedings, his devoted time and his ideas has enabled me to make the project a success. His faith in me has always made me more confident and aggressive. It was my privilege to work under his guidance.

I would like to thank **Dr. Kulvir Singh**, assistant professor, School of Physics and Material science for his full motivation and appreciation to my work. My greatest thanks to **Dr. Maneek Kumar**, Prof and Head, Department of Civil Engineering for helping me throughout my M.Tech. I am greatful to him for sharing his time and expertise. I would like to thank research scholars **Mr. Manoj Sharma, Mr. Akshay, Mr. Vishal and Mrs. Bhupinder Kaur** for kind help and valuable suggestions whenever I needed for creating a healthy research environment.

My special thanks to laboratory superintendent **Mr. Purushottam**. His assistance and partnership were of great pleasure. I would also like to thank **Mr. Jant Singh**, for providing all kind of assistance in PG Lab. All the faculty, my friends and colleagues are anknowledged for providing me a friendly atmosphere. My most profound thanks to my parents who are always with me in my difficult time. Thanks to my friends **Mr. Varun** (London) and **Mr. Atul** (Melbourne) for being with me always to help me out. Above all, my special thanks to my fiancée **Ms. Sakshi Khosla**, who inspired me to do more and more hard work and keeping an immense faith in me for my wonderful future.

Raj Kumar Chopra

RAJ KUMAR CHOPRA

Dedicated to my Loving Parents

LIST OF TABLES.....

LIST OF FIGURES.....

LIST OF ABBREVIATIONS

SEM	Scanning electron microscopy
TEM	Transmission electron microscopy
WC	Tungsten Carbide
$C_3H_8O_3$	Glycerol
WO_3	Tungsten oxide
XRD	X-Ray Diffraction

ABSTRACT

Tungsten Carbide (WC) is one of the hardest material used in cutting tool industry and also as a coating material. Fine and uniform distribution of tungsten carbide in the ductile metal matrix can give remarkable results like longer tool life. By reduction in size from micro to nano scale materials show different properties because of the high surface to volume ratio. High hardness and better toughness can be obtained by synthesizing particles of tungsten carbide in nano dimensions. Nano-grained WC/Co composites have the potential to become the new materials for tools and dies and wear parts. Shorter sintering time, high purity, and precise control of composition are the benefits of nano-grained WC/Co particles. These materials have superior properties with more homogeneous microstructure than conventional WC/Co composites. Higher toughness and ductility can be achieved without reducing hardness and wear resistance. In the present investigation thermo-chemical route using reflux action technique for the synthesis of tungsten carbide nano particles has been adopted. The synthesized powder is characterized by X-Ray diffraction and TEM technique. The detail of the synthesis and characterization work is presented in this thesis. During design of experiments several failure occurred which could not give desired results. In this work only those experiments are reported which could deliver the desired results.

INDEX

CONTENTS **PAGE NUMBER**

CHAPTER – 1 *INTRODUCTION*

1.1 Introduction

Cemented tungsten carbide is one of the oldest and most successful powder metallurgy products which have its commercial applications in cutting tool industry [1]. Exceptional hardness with good wear/erosion resistance are the basic properties of WC which makes it suitable as a cutting tool substance. Cutting tools must be able to resist high temperature and severe temperature gradients, thermal shock, fatigue, abrasion, attrition, and chemical induced wear. Thus materials for cutting tools and dies must have high hardness to combat wear, hot strength to overcome the heat involved, and sufficient toughness to withstand interrupted cuts or vibrations occurring during the machining process. Cutting tools are a two billion-dollar industry worldwide and form the backbone of manufacturing operations for metals, polymers, and advanced materials such as intermetallics and composites of all types [2, 3].

Tungsten carbide (WC) has been well known for its exceptional hardness and wear/erosion resistance. Ductile metals, such as cobalt, which act as binder greatly, improve its toughness so that brittle fracture can be avoided. These composites are essentially aggregates of particles of tungsten carbide bonded with cobalt metal via liquid-phase sintering. The properties of these materials are derived from those of the constituents namely, the hard and brittle carbide and the softer, more ductile binder. The cutting tool and wear part applications arise because of their unique combination of mechanical, physical, and chemical properties. Although other metal carbides, such as TiC, are also used in cutting tools, around 95% of all cemented-carbide cutting tools are tungsten carbide-based [1]. In 1992, 60% of metallic tungsten produced went into WC for cutting tools, dies, etc., only 25 % went into lamp filaments, heating elements, and mill products, with most of the remainder was used in steels and super-alloys [4]. Annual production of tungsten for use in tungsten carbide worldwide was about 25,000 metric tons in 1991-92 [5]. The traditional method of making WC-Co cemented carbide is by crushing, grinding, blending and consolidation of the constituent powders. In this way the distribution of WC in ductile matrix find its limited approach where its size cannot be reduced further as compared to the size of milled powder which is typically 1-10 micron in diameter on microscopic scale. However, efforts have been made to obtain fine distribution of WC in the ductile matrix. With great efforts, the micro

structural scale can be reduced to about 500nm [4]. Nano crystalline ceramic materials were found to have higher hardness, fracture toughness and ductility and are sintered at lower temperature and pressure than coarse-grained powder [5]. It is therefore expected that the properties of cutting tools (to resist high temperature and severe temperature gradients, thermal shock, fatigue, abrasion, attrition and chemical induced wear) can be improved by lowering the grain size into nano scale [6, 7].

1.2 The Discovery of Tungsten Carbide

Henri Moissan (1852-1907), a Nobel Laureate (1906), is best known as the inventor of electric furnace and for his unsuccessful attempts to prepare artificial diamonds. It was in the laboratory in a school of pharmacy at the University of Paris where the two carbide of tungsten were discovered namely W_2C (1896) by H. Moissan and WC (1898) by P.Williams [8]. The first commercial tungsten carbide products were melt cast for wire-drawing dies. Unfortunately, the cast pure WC was quite impractical in nature because the stiochiometric compound WC, with 6.13 weight % carbon, does not melt congruently. This decomposes to a fragile mixture of W_2C, WC and graphite upon cooling. However, at lower carbon contents, mixture of WC and W_2C are formed on cooling, which melt at a relatively moderate temperature, around 2750°C. The resultant cast product was very hard and brittle, but very much usable for some application such as dies. The first sintered tungsten carbide was produced in 1914 for use in drawing dies and rock drilling. It was developed in an attempt to avoid the casting defects common to the molten product, and consisted of powder tungsten carbide or molybdenum carbide or mixture of both, which were pressed and then sintered just below the melting temperature of the pure WC. However, the sintered product was very brittle and unsuccessful in industry for its further use [8].

1.3 Tungsten Carbide Phase Diagram

WC is a compound comprising of W and C elements. The reaction of W with C leads to formation of several compounds. These reactions do occur at different temperatures with variation in C content. An equilibrium reaction between W and C may provide the path for formation of different phase. The existence of equilibrium phases at different composition and temperature is shown in binary phase diagram (W-C) (fig.1.1). The binary phase diagram

of W-C shows three stoichiometries, hexagonal W_2C crystallizing in three modifications the PbO_2, Fe_2N and CdI_2 types, denoted by β, β ' and β " respectively, the cubic sub-carbide WC_{1-x} crystallizing in the NaCl type structure denoted by gamma, and the hexagonal WC denoted by δ. W_2C exhibit a comparatively wide homogeneity range of 25.5 to 34 at % C at 2715°C. This phase originates from a eutectoidal reaction between elements W and δ-WC at 1250°C and melts congruently with the W solid solution at 1715±5°C and with WC_{1-x} at approximately 2758°C [7]. Phases of W_2C stoichiometry are obtained as intermediate products during WC production. The gamma- phase results from a eutectoid reaction between β and δ at 2535°C which melts at approximately 2785°C. It can be obtained at room temperature by extremely rapid cooling e.g. in plasma sprayed layers. The technically important δ-WC is the only binary phase stable at room temperature and has almost no solid solubility up to 2384°C but may become carbon deficient between this temperature and its incongruent melting point [8]. The monocarbide WC has a simple hexagonal crystal structure with two atoms per unit cell and a c/a ratio of 0.976 [8]. The stable structure of tungsten is body centered cubic (α-W) but a second form α-W has long been recognized which is stable at temperature below 650°C with cubic structure. β-W phase was first observed in dendritic metallic deposits, formed on cathode after electrolysis of phosphates metals below 650°C [9]. Hydrogen reduction of WO_3 at T ≤ 575°C is the most direct method of obtaining x-ray pure β-W, [10].

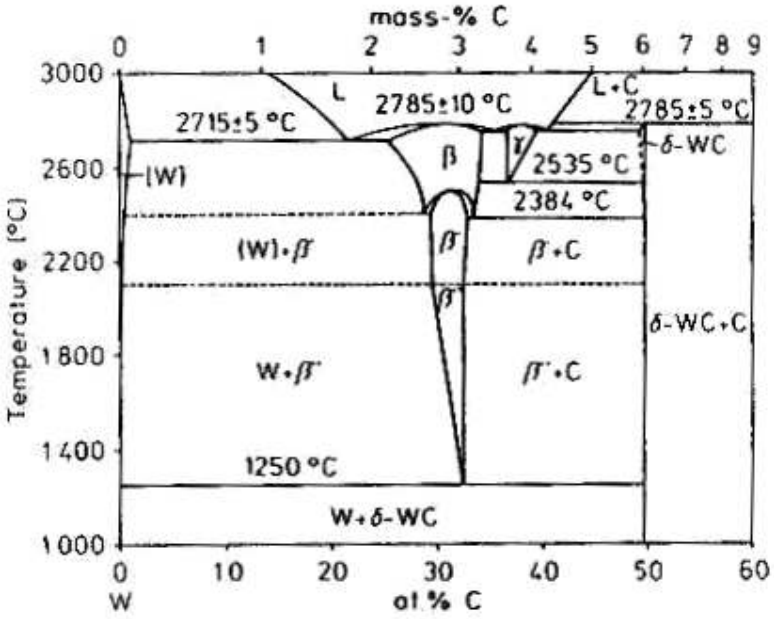

Figure1.1: Phase diagram of tungsten carbide

1.4 Cemented Carbide

Cemented tungsten carbide originated in the electric incandescent lamp industry in the US and in Germany. Since the invention of tungsten filaments for use in incandescent lamps at the beginning of the 20th century, the lamp manufacturers had been searching for a replacement for the expensive diamond dies used in the wire-drawing of fine tungsten filaments. Prompted by a strategic shortage of industrial diamonds at the beginning of World War I, the German lamp industry turned to the tungsten carbides as potential substitute materials. Because of their extreme hardness, the carbides of tungsten initiated a substantial research and development effort on the part of the incandescent lamp industry and their suppliers, for more than two decades. A major breakthrough took place with the advent of cemented tungsten carbide in the 1920's. The successful development of the cemented carbides was generally attributed to the work of Karl Schrter who was a chemist [6]. At the beginning of World War I, he began searching for substitute materials for diamond in tungsten-wire-drawing equipment, starting with cast and sintered tungsten carbides. But neither the sintering process nor the casting processes for making tungsten carbide wire-drawing dies were deemed successful and the work was abandoned. It was resumed about 1920 at Osram. Systematic experiments to bind powdered tungsten carbide with iron, nickel or cobalt were carried out from 1918 to 1923. The first sintered cemented carbide dies were prepared in 1922. The wire-drawing tests showed cobalt to be the best additive. The invention of the cemented carbide tool materials was first disclosed in 1923 in Karl Schrter's patent application [11]. The two inventions claimed by the patent were: a unique hard metal alloy composition, namely the combination of the very hard tungsten carbide, WC, with small amounts of a metal of the iron group: iron (Fe), nickel (Ni) and cobalt (Co); and the manufacture of the hard metal alloys by the application of the process of powder metallurgy, namely the pressing and sintering of mixed powders of tungsten carbide and binder metal. The manufacturing process, then and now, is one of powder metallurgy, with liquid phase sintering. Karl Schrter's "decisive step" consisted of sintering a mixture of 90 wt% tungsten carbide and 10 wt% binder metal, namely Fe, Ni or Co, but preferably cobalt, at temperatures at which the binder is liquid and complete consolidation of the compact occurs. The resulting microstructure consists of an aggregate of fine (1-2 micrometers) WC particles embedded in the cobalt-rich binder. The properties are controlled by composition and microstructure: the

hardness increases with decreasing Co content and smaller particle size of WC, but, in general, at some cost of rupture strength and fracture toughness. The result was what we now known as "cemented carbides," a class of materials having distinctive microstructure and superior physical properties. The importance of the invention is confirmed by noting that today, seventy years later, the same compositions, made by essentially the same process, are still a very significant product of the tool materials industry. In tungsten-wire plants, the cemented carbide drawing dies quickly replaced diamond dies for reducing heated tungsten wire in the coarse range, after the swaging operation, i.e. from about 0.7 mm down to 0.3 mm in diameter. Significant as it was for wire-drawing dies, the new material represented a truly revolutionary cutting tool material for machining. The addition of cobalt to tungsten carbide not only allows the sintering of dense compacts at reasonable temperatures, but also results in materials with adequate toughness at very high hardness levels. When the new tools, made from sintered WC-Co, were placed on the market in 1927, they caused a sensation in the machine tool industry, by allowing cutting speeds 3 to 5 times faster than the best high speed steel tools in use at that time. Modification of Schrter's compositions by replacing either a portion or all of the tungsten carbide with other carbides (in particular those of titanium, tantalum, and molybdenum) led to the major discovery that such additions were essential for cutting steel at speeds that provide economic advantages. The discovery by Schwarzkopf that solid solutions of carbides are superior to individual carbide was the starting point of the development of multi-carbide cutting tools for high-speed machining of steel [12]. The most important advance in cutting tool technology since the development of WC-Co was the development of coated tools in late the 60's and early 70's. Coatings are diffusion barriers, and they prevent the interaction between the chip formed during machining and the cutting material. Typical coatings are titanium carbide (TiC), titanium nitride (TiN), titanium carbonitride (TiCN), and alumina (Al_2O_3), which are extremely hard, thus very abrasion resistant. TiN has the added advantage of a significantly lower coefficient of friction against steels compared to WC/Co. Thus it reduces the energy needed during the cutting operation. All these compounds have extremely low solubility in iron and they enable inserts to cut at much higher speeds than is possible with uncoated cemented carbides.

1.5 Properties of Tungsten Carbides

The key factor for the properties of WC-Co composites are the composition and the crystal structure [1]. Deviation from the ideal composition (carbon content) leads to the occurrence of either graphite or ternary compound. Both of these are undesirable, and results in degradation of mechanical properties and cutting performance. Therefore the carbon content must be maintained within narrow limits to obtain the desired composition with optimum properties as shown in figure (1.2). Table 1.1 presents some physical and mechanical properties of cemented carbide material.

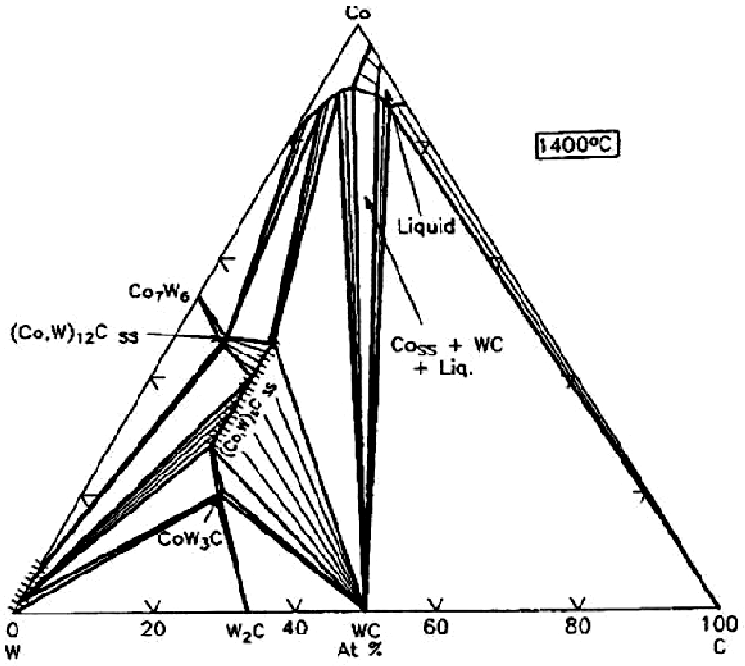

Fig 1.2: The isothermal section of WC-Co phase diagram at 1425 °C

TABLE 1.1: Properties and representative grade of cemented carbide [13]

Cemented carbide	**Room Temperature hardness, (HV)**	**Modulus Of elasticity, (GPa)**	**Transverse rupture strength, (MPa)**	**Coefficient of thermal expansion, (10^{-6}/K)**	**Thermal conductivity, (W/mK)**	**Density, (g/cm^3)**
WC-20 wt% Co	1050	490	2850	6.4	100	13.55
WC-10 wt% Co	1625	580	2280	5.5	110	14.50
WC-3 wt% Co	1900	673	1600	5.0	110	15.25

WC10wt%Co22wt %(Ti,Ta,Nb)C	1500	510	2000	6.1	40	11.40

Compared to other refractory carbides, the thermodynamic stability of tungsten carbide is relatively low, as its room-temperature hardness. At high temperatures, most cubic carbides rapidly lose their hardness, whereas the hardness of the WC is quite stable. Coupled with this fact, the unique deformation characteristics of WC are the basis for its predominance as the hard refractory phase in cemented carbides. Other noteworthy properties of WC are its extremely high modulus of elasticity, second only to that of diamond, and its high thermal conductivity. The other refractory carbides have been used effectively as grain growth inhibitors in liquid phase sintering of WC-Co. It has been found that the effectiveness of a transition metal carbide as a grain growth inhibitor is related to its thermodynamic stability, and they may be ranked as follows:

$$VC > Mo_2C > Cr_3C_2 > NbC > TaC > TiC > Zr/HfC$$

It was also found that there is a maximum level above which no further grain growth inhibition occurs. This level is believed to correspond to the maximum solubility of the carbide phase in liquid cobalt. A liquid phase that is saturated with inhibitor carbide would reduce the solubility of WC, and thereby reduce its coarsening rate. Table 1.2 lists properties of refractory carbides and binder metals [14].

TABLE 1.2: Properties of refractory metal carbides and binder materials [14]

Material	Hardness HV (50 Kg)	Crystal Structure	Melting Temperature	Theoretical density (g/cm3)	Modulus of elasticity GPa	Thermal expansion
WC	2200	Hexagonal	2800	15.63	696	5.2
W_2C	3000	Hexagonal	2777	17.3	_	_
TiC	3000	Cubic	3100	4.94	451	7.7
VC	2900	Cubic	2700	5.71	422	7.2
HfC	2600	Cubic	3900	12.76	352	6.6
ZrC	2700	Cubic	3400	6.56	348	6.7
NbC	2000	Cubic	3600	7.8	338	6.7
TaC	1800	Cubic	3800	14.50	285	6.3

Cr_3C_2	1400	Orthorhombic	1800	6.66	373	10.3
Co	<100	Cubic/Hexagonal	1495	8.9	207	16
Ni	<100	Cubic	1455	8.9	207	15

The role of cobalt in cemented carbides is to provide a ductile bonding matrix for tungsten carbide particles. Cobalt is used as a bonding matrix because its wetting or capillary action during liquid phase sintering allows the achievement of high densities. Because of the relatively high cost of cobalt, attempts have been made to design alternate materials, with iron and nickel as the predominant cobalt substitutes. However, sliding wear tests show that cobalt content is very important for cemented carbides to have good wear resistance.

Fracture in WC/Co systems with high Co contents has been found to occur mainly by the ductile rupture of Co through void nucleation and coalescence. Other fracture modes such as fracture along WC/Co interface and WC/WC grain boundary decohesion as well as cleavage across WC grains were also noted. These mechanisms occur especially at low volume fractions of Co binder in the composite at which the contiguity of WC grains begin to increase. The effect of the contiguity of WC skeleton on fracture toughness has also been demonstrated. In a fracture toughness experiment, in a given crack plane, the crack propagation is easy along the relatively weak WC/Co and WC/WC boundaries and final fracture is primarily controlled by the area fraction of Co regions intact across the crack plane ahead of the tip. Since the WC/WC decohesion and WC/Co interface fracture energies are likely to be lower than the fracture energy absorbed in ductile fracture of the binder, ductile failure of Co can be considered as a primary mechanism manifesting the fracture resistance. Several investigations attempted to correlate the microstructural parameters and mechanical properties of constituent phases to experimentally measured fracture toughness values.

In particular, it has been universally found that the fracture toughness increases with volume fraction, the mean free path length of the binder and the size of WC grains. In addition, higher toughness has been suggested to result from the increased contiguity of Co binder, which minimizes the fracture along weak WC/WC boundaries. For a given volume fraction, geometrical arrangement of the ductile binder as a continuous thin matrix phase is beneficial for high toughness while retaining high strength. This arrangement could be most desirable of several possible arrangements in which the deformation of ductile Co phase is highly constrained in the microstructure.

1.6 Nano Materials Research

Nanoscale particle research has recently become a very important field in materials science. Nanoscale particles (1 to 100 nm) usually have physical properties different from those of large particles (10-100 nm) or the molecular/atomic species. It has been found that nanoparticles exhibit a variety of previously unavailable properties, depending on particle size, including magnetic, optical, and other physical properties as well as surface reactivity [15]. Recent experiments have shown that consolidated nano-materials have improved mechanical properties, such as increased hardness of metals and increased ductility and plasticity of ceramics. The unique properties of nanoscale particles and nano grain bulk materials can be attributed to two basic phenomena. The first is that the number of atoms at the surface and/or grain boundaries in these materials is comparable to that of the atoms located in the crystal lattice, thus the chemical and physical properties are increasingly dominated by the atoms at these locations. The second phenomenon is the "quantum-size effect" or quantum confinement effect. When particles approach the nanometer size range, their electronic and photonic properties can be significantly modified as a result of the absence of a few atoms in the lattice and the resulting relaxation of the lattice structure. The worldwide cemented carbide cutting tool industry has approached the problem of higher mechanical properties for their cutting tools by altering composition primarily in the direction of increased carbide content. Unfortunately, at the level of 94 to 97 weight percent carbides, fracture toughness and strain tolerance have fallen below acceptable levels and excessive brittleness results. One answer to this dilemma is to reduce the average particle size of the hard carbides, thus reducing the mean free path between carbide particles. This usually has the effect of increasing fracture toughness as well as wear resistance. The latter effect is achieved because the matrix is now exposed to the abrasive/corrosive environment over much smaller dimensions, even though the WC/Co composition has not changed. By means of this particle size reduction process, the fracture toughness and strength can be increased significantly, as long as two other deleterious effects have not been introduced. These are:

- Excessive impurities such as oxygen during the very long milling times necessary for mechanical mixing, and
- Establishment of WC-WC particle contact, especially over distances spanning many WC particles, thus creating a brittle fracture initiation site and propagation path.

These two problems will negate any increase in fracture toughness in other portions of the volume of the tool. These effects limit the cost-effective mechanical milling reduction of particle size and proper WC/Co dispersion to a typical average WC size of 0.5 to 1.0 micron. The most striking is the abrasion resistance, with finer grain composites (still in micron range) having much better abrasion resistance.

1.7 Applications

Cemented carbides, best known for their superior wear resistance, have a range of industrial uses which are diverse compared to other powder metallurgy product applications. Common uses include metalworking tools, mining tools, and wear resistant components. All of these applications have one physical property requirement in common: the ability to resist wear. The performance of cemented carbide as a cutting tool lies between that of tool steel and "cermets" [20]. Compared to tool steels, cemented carbides are harder and more wear resistant, but also exhibit lower fracture resistance and thermal conductivities than tool steel. Cermets, which are composed of carbonitride based materials such as TiCN, on the other hand are more wear resistant than cemented carbides, but may not be as tough.

Advances in cemented carbides have produced a wide selection of tool materials. They are suitable to cut a variety of materials such as gray cast iron, ductile nodular iron, austenitic stainless steel, nickel-base alloys, titanium alloys, aluminium, free-machining steels, plain carbon steels, alloy steels, and martensitic and ferrite stainless steels. Almost 50% of the total production of cemented carbides is now used for non metal cutting applications such as drill bits and components for mining, oil and gas drilling, transportation and construction, metal forming, structural and fluid-handling components, and forestry tools [20]. New applications are constantly being identified for carbides, largely because of their excellent combinations of abrasion resistance, mechanical impact strength, compressive

strength, high elastic modulus, thermal shock resistance, and corrosion resistance. Erosion resistance of carbides is important in applications such as sand blast/spray nozzles, seals in slurry pumps, and component parts in the oil industry. Cemented carbide is an excellent choice for the nozzles because it can outwear steel 100 to 1 and will thereby maintain the spray pattern and quantity of flow for a longer period of time, extending the service life of the nozzles. Many applications can use a small carbide nozzle insert held to other base materials by epoxy, braze, and shrink fit or taper fit. This permits the use of carbide without a major redesign of a nozzle assembly or the need to manufacture a complex shape from solid carbides. In the mining and mineral industries, the components exposed to severe mechanical interaction among very abrasive non metallic and metallic materials. The abrasive nature of most ores can cause significant wear to both handling and processing equipment. A variety of WC/Co materials have been used for hard facing to meet an extremely wide range of severe abrasive conditions, especially oil well drill bits, tool joints, rock drill bits.

The physical and mechanical properties of cemented tungsten carbides make them appropriate materials for a wide range of structural components, including plungers, boring bars, powder compacting dies and punches, high pressure dies and punches, pulverizing hammers, carbide feed rolls and chuck jaws, and many others. The predominant wear factors in most applications are high abrasion, attrition, and erosion. The rigidity, hardness, and dimensional stability of cemented carbide, coupled with its resistance to abrasion, corrosion, and extreme temperature, provide superior performance in fluid-handling application, such as seal rings, bearings, valve stems, and valve seats. Among the diverse applications of cemented carbides is a wide range of tools and components for the transportation and construction industries. Examples include tools for road planning, soil stabilization, asphalt reclamation, vertical and horizontal drilling, trenching, dredging, tunnel boring, and forestry, as well as snow-plow blades, tire studs, and street sweeper skids.

Erosion resistance of carbides is important in applications such as sand blast/spray nozzles, seals in slurry pumps, and component parts in the oil industry. The success of cemented carbides in erosion resistant application is again due to their unique composite structure of wear-resistant WC particles in a ductile cobalt matrix. WC-Co has also been used as coatings in jet engine parts such as fans and high pressure compressors (HPC). The materials used for fan and HPC blade interlocks in a jet engine are usually titanium alloys, which have poor wear properties. Most fan and HPC interlocks use thermal sprayed WC-Co

coatings or brazed-on WC-Co powder metallurgy wear pads to prevent excessive wear. The WC-Co coatings are successful in the titanium alloy interlock applications because of the following reasons.

- High wear resistance of the tungsten carbide,
- Adequate fracture toughness because of the cobalt matrix,
- High adherence on the titanium alloy substrates, and
- Good match in coefficient of thermal expansion with the titanium alloy substrate materials.

The typical range of temperatures for fan interlocks is from subzero to 95^0C in the fan and from 40 to 260^0C in the HPC. Fortunately, WC-Co coatings appear to retain sufficient low temperature ductility and high temperature oxidation resistance over these temperature ranges. The formation of a wear glaze at the contact zones contributes to the good wear resistance of the WC-Co in the interlock applications. The WC-Co coatings have also been used in other engine components such as nozzle assemblies. The titanium components in the exhaust nozzle generally have poor wear resistance and almost always require coatings on mating parts in relative motion. Oxidation of the carbide limits use of this coating to temperatures below 480^0C. Nano grained WC/Co composites are expected to enter the above mentioned areas. With both high hardness and high toughness, new applications for nano grained WC/Co composites are also expected to be found.

CHAPTER – 2 *LITRATURE REVIEW*

McCandlish L.E., Kear B.H. and Kim B.K [22] reported the thermo chemical synthesis method of WC-Co nanoparticles. With traditional methods of synthesis WC embedded in cobalt matrix typically (1-10 μm) sized particles can be achieved. To reduce the particle size to nano scale one of the initial methods was thermo chemical synthesis method. In this approach one has to start with a precursor compounds in which W and Co are mixed at the molecular level, and then to transform these compounds into nanostructured WC-Co powder by thermo chemical treatment.

Various steps followed in thermo chemical synthesis are:

- Precipitation of molecular precursor powder (W_3O) at 100°C thereby mixing W and Co at molecular level.
- Reacting precursor powder at controlled carbon and oxygen activity at 600 to1000°C to produce nano structured WC-Co powder.
- Addition of lubricant and to press to shape by cold compaction.
- HIP- sinter at 1200°C.

A prerequisite is a homogeneous precursor powder, in which W and Co are intimately mixed at molecular level, such as in the compound tris(ethylenediamine) cobalt tungstate, $Co(en)_3WO_4$, which after reduction and carburization yields WC-23 wt% cobalt . Other composition (i.e. W/Co ratios) can be obtained from aqueous solution mixture, such as Co $(en)_3WO_4$ + H_2WO_4 or AMT + $CoCl_2$ (where AMT= $(NH_4)_6(H_2W_{12}O_{40}).4H_2O$. These solution, upon atomization and rapid drying, precipitate homogeneous powder with amorphous or micro crystalline structure, which are suitable precursors for subsequent thermo chemical processing to the desired nanostructure WC-Co powder. Spray dried powders have been used to produce WC-Co powders with from 3- 30 wt % Co. Reduction of

Co $(en)_3WO_4$ powder in 1:1 H_2: Ar gas, as the powder is heated from room temperature to 700°C at the rate of 25°C / min. The ethylenediemine ligands are cleanly removed at between 150-250°C and reduction is complete at 650°C. The result of this reduction process is a nanostructured powder. Consolidation of powder is done by liquid phase sintering. However, it is necessary to minimize the time spent at the sintering temperature in order to minimize particle coarsening; tests have shown that dense structures in WC-Co Wt% Co can be achieved in 30 seconds at 1400°C which gives WC grain size of about 200nm. An additional 30 second sintering time increase the WC grain size to 2.0 microns. A small amount of uncombined C or an addition of Cr inhibits grain growth during liquid phase sintering. Ultra pure WC-Co powders can be consolidated by solid state sintering, where grain growth is much slower. Critical to the success of the process is the control of thermodynamics and kinetics of gas-solid reactions in a field bed reactor. A low sintering temperature and a short sintering time insure reaction of a nanostructure in consolidated material.

Zhu Y. T. and Manthiram A [23] reported the synthesis of WC-Co nano composite from ammonium tungunstate using a polymer as carbon source. Use of a polymer as an in situ carbon source reduces the diffusion length and become particularly attractive for large scale production. Procedure involve the mixing of ammonium tungunstate and cobalt nitrate, decomposition in air on a hot plate, dispersion in a dimethylformamide (DMF) solution of polyacrylonitrile and firing in Ar-H_2 mixture at 800-900°C which yield WC. Addition of aqueous cobalt acetate in it and evaporating the solvent we get a black mass which fired at 400°C for 4 hour in a mixture of 90% Ar-10% H_2 gives the final product.

Geo L. and. Kear B.H [24] studied the synthesis of nanophase WC powder by a displacement reaction process. It is a novel displacement reaction process which combines reduction and carburization of ammonium or tungsten oxide in a single operation. The critical step in the process is the heating rate, which should be slow enough to ensure a balance between reduction and carburization kinetics. The process is a one step process, a gas phase mixture of H_2/Co (2:1) or (1:1 molar ratio) is passed over the heated tungsten base precursor powder at temperature upto 700°C in order to affect its direct conversion to nanophase WC. (Fig 2.2)

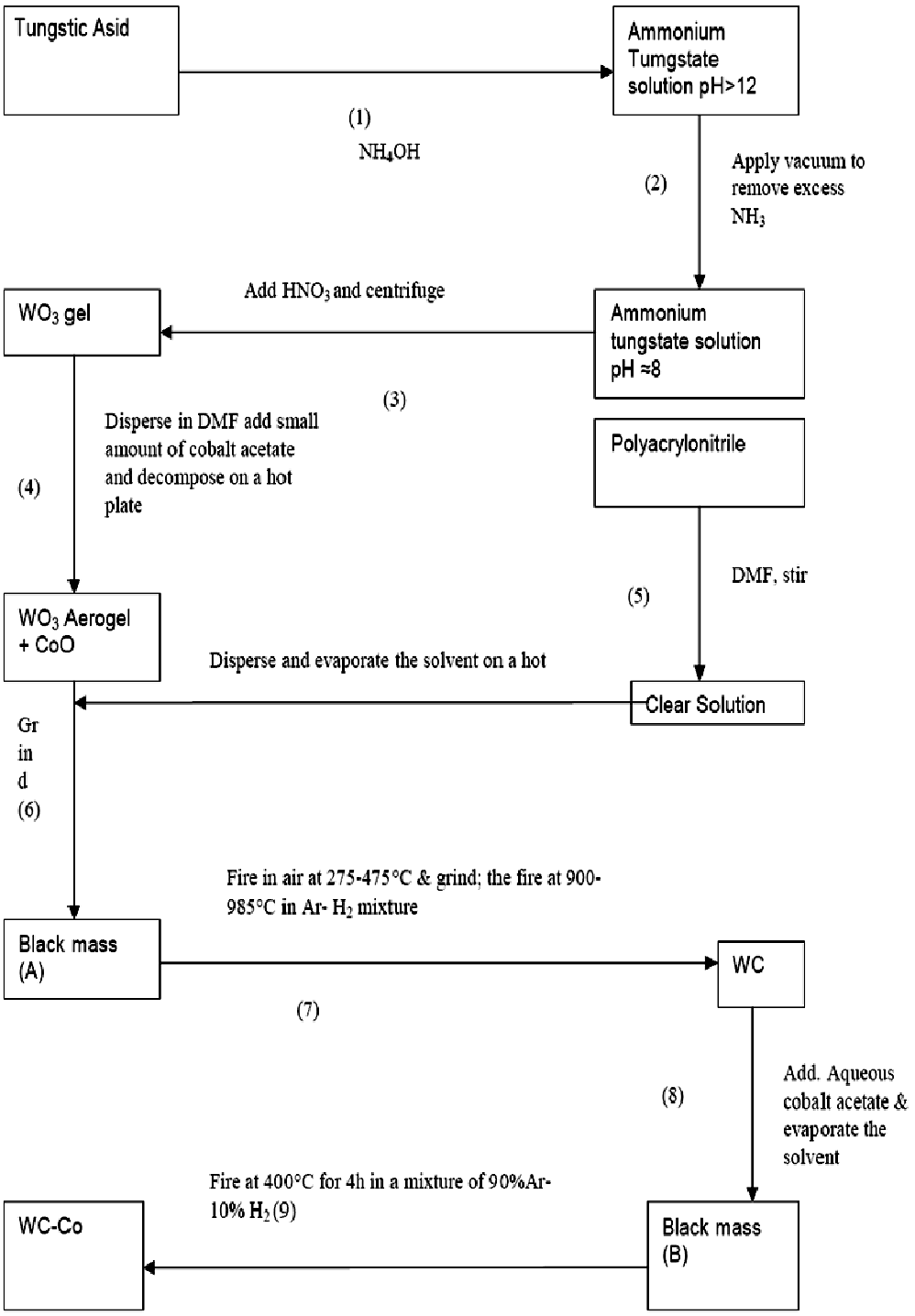
Tungstic Asid
Ammonium Tumgstate solution pH>12
(1)
NH_4OH
(2)
Apply vacuum to remove excess NH_3
WO_3 gel
Add HNO_3 and centrifuge
Ammonium tungstate solution pH ≈8
(3)
Disperse in DMF add small amount of cobalt acetate and decompose on a hot plate
(4)
Polyacrylonitrile
DMF, stir
(5)
WO_3 Aerogel + CoO
Disperse and evaporate the solvent on a hot
Clear Solution
Gr in d (6)
Fire in air at 275-475°C & grind; the fire at 900-985°C in Ar- H_2 mixture
Black mass (A)
WC
(7)
(8)
Add. Aqueous cobalt acetate & evaporate the solvent
Fire at 400°C for 4h in a mixture of 90%Ar-10% H_2 (9)
WC-Co
Black mass (B)

Fig. 2.1: Synthesis of WC-Co nano composite using polymer as carbon source

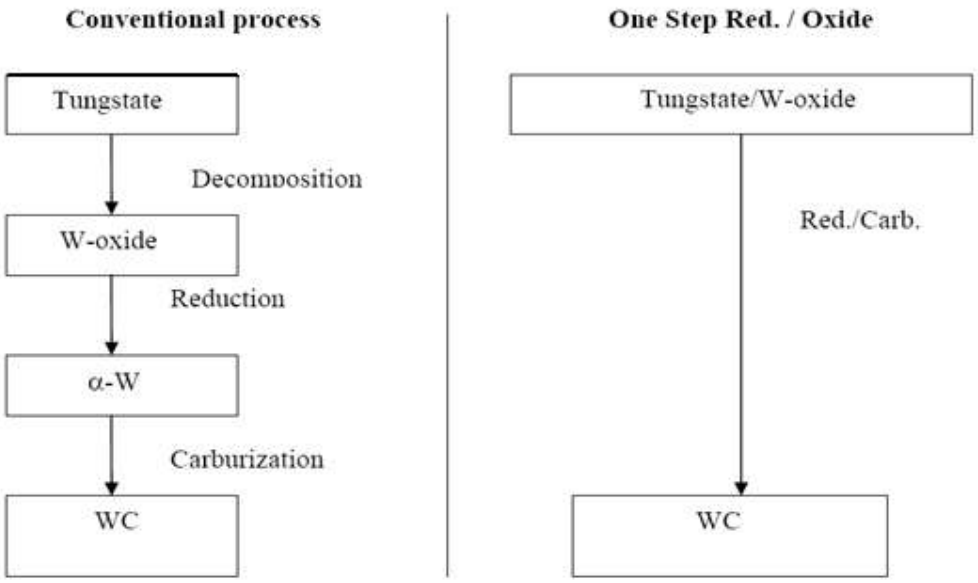

Fig. 2.2: Synthesis of nanophase WC powder by displacement reaction

The proposed displacement reaction process involving the formation of an intermediate oxycarbide phase. The initial nanophase tungsten oxide particle is reduced by H_2 through the formation of H_2O at its surface. As the H_2O molecules are removed by the flowing gas stream, the active tungsten sites react with the Co to form an incipient oxy-carbide phase, liberating CO_2 that is also carried away by the flowing gas stream. Further reaction gradually transforms the oxy-carbide into nanophase WC. In this case the formation of metastable W_2C phase is avoided.

BAN Z. G. and Shaw L.L [25] reported the synthesis of nanostructured WC-Co powder by integrated mechanical and thermal activation (IMTA) process. As a result of integrated mechanical and thermal activation (IMTA), nanostructured WC-Co powder is synthesized below 1000°C starting from WO_3, CoO and graphite powder mixture. Consolidation of nanostructured WC-Co powder is done via. High velocity oxy-fuel (HVOF) thermal spraying and solid state sintering .The powder mixture prepared containing WO_3, C and CoO with a molar ratio of 1:2.4:0.7 in order to form the final product of WC+18 wt. % Co+5.3 wt. %C. This powder mixture was high energy milled for different times. The

mechanically activated (high energy ball milled) powder was subsequently subjected to thermal activation. The thermal activation was carried out by heating the milled powder at 650°C for 2h in a gas mixture of H_2 (P_{H_2}=0.5 atmosphere) and Ar (P_{Ar}=0.5 atmosphere), followed by ramping to 1000°C and holding at this temperature for 2 h in pure argon (P_{Ar}=1 atmosphere), free carbon is often present in the nanostructured WC-Co powder obtained from the IMTA process (Fig. 2.3) because of the extra carbon added in the beginning of the process. To control the free carbon concentration in the gas synthesized WC-Co powder, a gas mixture of CO/CO_2 was used to purify the powder at a chosen temperature after thermal activation. Consolidation of the resulting nanophase WC-Co powder is done by high velocity oxy fuel (HVOF), thermal spraying and free sintering to prepare coating and bulk samples respectively. Sintering of WC-Co is highly affected by carbon content. By using the CO/CO_2 treatment, the concentration of free carbon in the nano powder has been kept bellow 0.05wt. %, . The resulting powder has a narrow particle size distribution (0.3 to 0.5 μm) and the crystal size of the WC phase is about 30 nm.

Michael J. Hudson, John W. Peckett, and Peter J.F. Harris [26] reported the synthesis of ordered nanoparticles of WC via. low temperature SOL-GEL . Tungsten carbide particles have been prepared by the gel precipitation of tungstic acid in the presence of an organic gelling agent 10% ammonium poly (acrylic acid) in water.

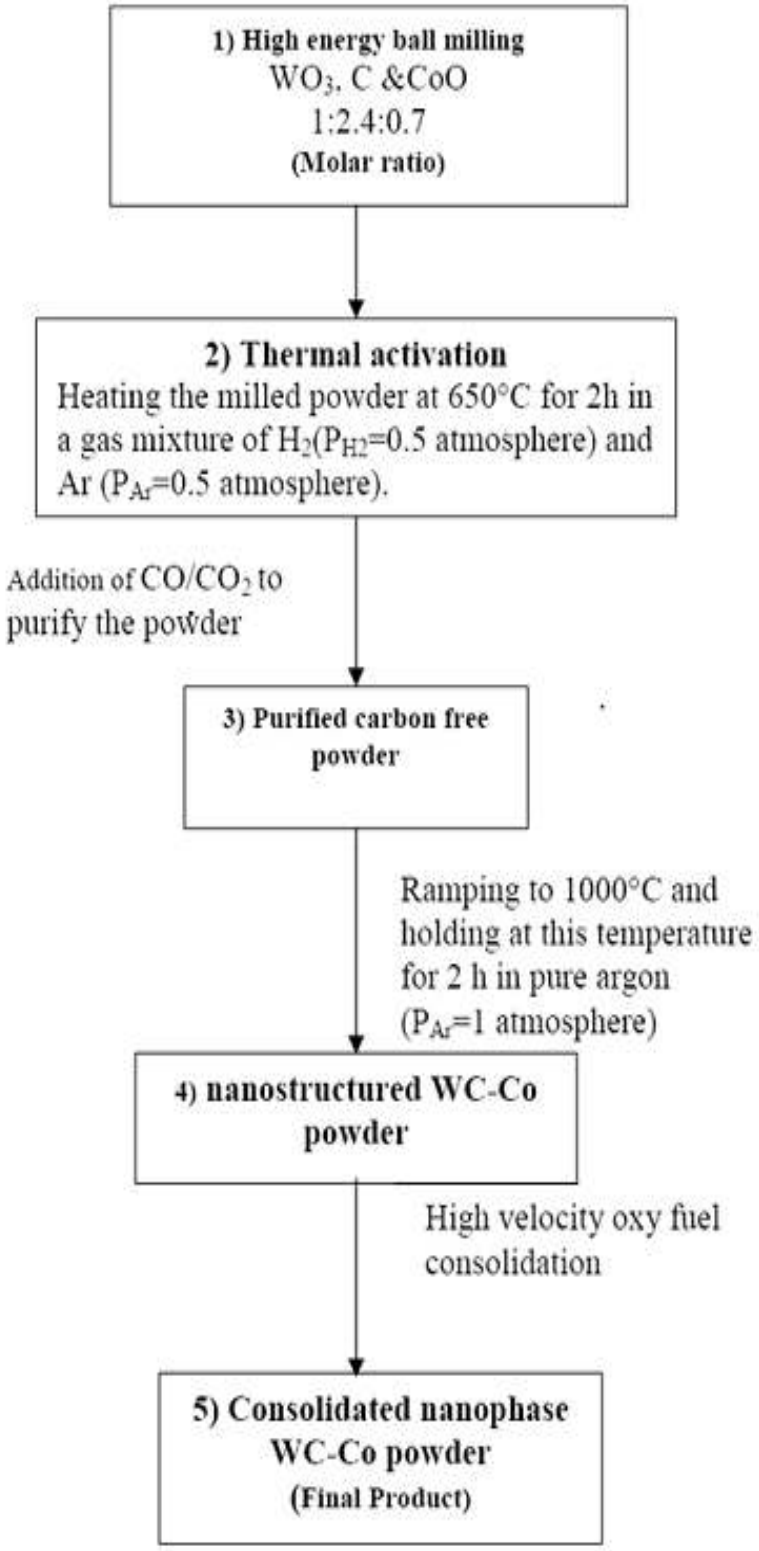

Fig 2.3: Synthesis of nanostructured WC-Co powder by integrated mechanical and thermal activation (IMTA) process

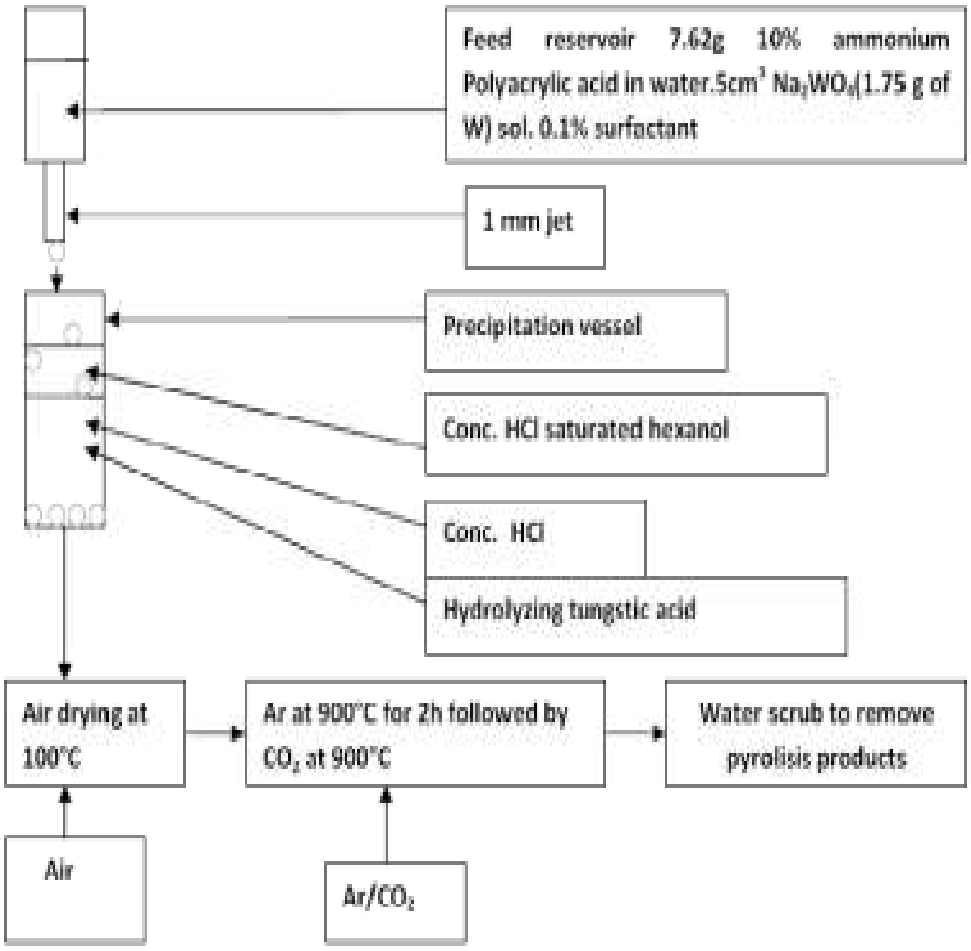

Fig. 2.4: Synthesis of nanoparticles of WC via low temp. SOL-GEL method

The feed solution, a homogeneous of sodium tungstate and ammonium poly(acrylic acid) in water, was dropped from a 1mm jet into hydrochloric acid saturated hexanol/concentrated hydrochloric acid to give particles of mixture of tungstic acid and poly(acrylic acid) which after drying in air at 100°C and heating to 900°C in argon for 2 h, followed by heating in carbon dioxide for a further 2 h and cooling, gives a mixture of WO_x, WC and traces of Na_xWO_3 with the carbon for the formation of WC being provided by the thermal carbonization of poly(acrylic acid). A flow sheet of the process is presented in the figure 2.4.The product after solidification for 40 min in water, consists of mainly nanoscopic tungsten carbide with a particle size of < 40 to 75 nm.

Jadambaa Temuujin, Mamoru Senna, Tsedev Jadambaa and Dondog Byambasuren [27] reported the synthesis of tungsten carbide nanoparticles by mechanically assisted carbothermic reduction natural wolframite. Carbothermic reduction of natural wolframite ($FeWO_4$) to nano sized tungsten carbide (WC) particles were achieved by calcining mechanically activated mixture of $FeWO_4$ and active carbon at 1100°C under flowing argon gas. The average particle size ranged between 20 to 25nm. Intermediate, Fe_6W_6C and Fe_3W_3C, were observed between 900°C and 1100°C, which decomposes to give the final product WC. Increased homogeneity with associated decrease in the diffusion path by milling are mainly responsible for the successful production of WC. The starting material $FeWO_4$ (WO_3:71.85, Fe_2O_3:20.36, MnO_2:5.46, SiO_2:1.1wt %) was ball milled to reduce particle size to 10 μm. Active carbon with their average particle size 35 nm is used here. The composition of the mixture was set equal to the stoichiometry of the reaction;

$$FeWO_4 + 5C \longrightarrow Fe + WC + 4CO$$

Well dispersed tungsten carbide nanoparticles of 20-25 nm were obtained from a direct carbothermic reduction from mechanically activated and homogenized mixtures comprising natural $FeWO_4$ and active carbon. The final product WC was formed via intermediate ternary carbide phases Fe_6W_6C and Fe_3W_3C. The well-crystallized WC contained only small fractions of impurities, i.e., Fe_3W_3C, Fe_7W_6, W, Fe_3C, and Fe. Milling just for 2 h was sufficient for practical full conversion to WC at temperature as low as 1100°C.

Chunli Guo, Lio Yi, Xiaojian Ma, Yitai Qian, and Liqiang Xu [28] reported the synthesis of tungsten carbide nanocrystals via a simple reductive reaction. Tungsten carbide nanocrystals had been prepared by the simple reaction of WO_3, Mg and anhydrous CH_3CH_2OH in an autoclave at 600°C. CH_3CH_2OH and WO_3 were used as carbon and tungsten source and Mg as the reductant. The overall reaction equation;

$$WO_3 + CH_3CH_2OH + 4Mg \longrightarrow WC + C + 4MgO + 3H_2$$

Approximate amounts of WO_3 (1.5g), Mg (1g) and anhydrous CH_3CH_2OH (12ml) were put in to a stainless steel autoclave of 16ml capacity. Then the autoclave was sealed and put

into a electric furnace at 100°C, the temperature of the furnace was increased to 600°C in 50 min and maintained at 600°C for 15 hour. Then, it was allowed to cool down to room temperature. The dark solid powder was collected and washed by dilute HCl to remove un reacted Mg powder. After that sample was washed with distilled water and ethanol to eliminate byproducts, and then it was dried in a vacuum at 50°C for 10 hour. Viewing the literature, we got several methods for the synthesis of WC-Co nanocomposites. The method "Thermo chemical Synthesis" is used for commercial production of nanostructured WC-Co composites. The benefit of the process is, low sintering temperature and short sintering time which ensures retention of nanostructure in the consolidated material. Additional 30 second's sintering time increase the WC grain size from nano scale to micro scale. The second method is very sensitive to production parameters; for example

- The initial mixing of ammonium tungstate and cobalt nitrate leads to the formation of $CoWO_4$ which can facilitate the formation of unwanted Co_6W_6 phase and
- The thermal degradation of polyacrylonitrile occurs over a range of temperature and is complex, which makes the firing temperature and time very critical in obtaining the desired product.
- Large quantity of sample leads to slower WC formation kinetics.

Third process is one step process which is advantageous but the limitation of this synthesis process is its heating rate which should be slow enough to ensure balance between reduction and carburization kinetics.

In IMTA process we can synthesize nanostructured WC-Co powder below 1000°C. Limitation of the process is the free carbon present in the bulk cemented carbide which reduces hardness and wear resistance, so here we have to utilize gas mixture of CO and CO_2 to control the amount of free carbon.

With "low temperature Sol- Gel Preparation method" also we can prepare nanostructured WC-Co below 1000°C. The main limitation of this process is that we have to handle the product very carefully while maintaining an atmosphere of CO_2 we have to cool it to room temperature because even if slightly warm the material gets red hot.

This synthesis route was very simple and easy to control and can be extended to synthesis other transition metal carbide.

Kumar A, Singh K and Pandey O. P [28] investigated the thermochemical route to synthesize WC nanoparticles from WO_3. The results indicate that reduction of WO_3 to WC takes place by absorption of carbon at the surface of WO_3 forming porous structure at the defect sites through which carbon diffuses. As the concentration of adsorbed carbon increases the growth of carbon nanotube starts from this site which ultimately gets converted to carbon nano fibers of higher chemical activity.

The powders of tungsten oxide (WO_3) and magnesium (Mg) were used as initial ingredients. The average particle size and purity of both the ingredients was 20 mm, 99.9 %, and 178 mm, 98% respectively. Magnesium powder was selected as reducing agent. Apart from this, either acetone or ethanol was used as a carbon source in the present study. All the chemicals were used in as received condition without further purification. The preparation of WC nano powders was carried out in a specially designed stainless steel autoclave of 50 ml capacity. Samples were synthesized using acetone and ethanol as carbon source respectively. Appropriate amount of WO_3, Mg, and anhydrous ethanol/acetone were put into a specially designed stainless steel autoclave. The sealed autoclave was kept into a resistance heating furnace. The temperature of the furnace was increased from room temperature to 600ºC with heating rate of 5º C/min. The autoclave was kept inside the furnace for 15 hours at 600ºC followed by furnace cooling of the autoclave. After the reaction is over, the dark solid powder was taken out from the autoclave and dissolved in HCl (1:1) to remove unreacted Mg and other soluble phases from the product. The acid treated samples were washed with distilled water first followed by ethanol to eliminate the water absorbed in the powders. The dried powders were characterized to investigate the formation of WC phase in the synthesized mass.

The possible reaction which may occur at high temperature and high pressure can be written as:

$$2WO_3 + 4CH_3COCH_3 + Mg \longrightarrow WC + C + MgWO_4 + 12H_2 + 3CO_2 \qquad (1)$$

$$2WO_3 + 2CH_3CH_2OH + Mg \longrightarrow WC + C + MgWO_4 + 6H_2 + 2CO_2 \qquad (2)$$

$$6\ CH_3CH_2OH + Mg \longrightarrow MgO + C_2H_6 \quad (3)$$

$$WO_3 + MgO \longrightarrow MgWO_4 \quad (4)$$

$$4C + 2WO_3 \longrightarrow WC + 3CO_2 \quad (5)$$

During synthesis pressure generated due to high temperature plays a major role for the conversion of WO_3 to WC. The liberation of ethane and hydrogen during course of synthesis leads to formation of carbon nano tube. Thermal analysis indicates that the product contains more carbon if ethanol is used as carbon source as compared to acetone.

D. D Wang and Montane. E Chornet [30] investigated the thermal cracking of glycerol and acetaldehyde pyrolysis products. Large numbers of primary and secondary pyrolysis products are generated through many different pathways. Partial thermal cracking of oxygenated hydrocarbons would produce hydrogen, carbon monoxide, carbon dioxide, methane and coke by primary decomposition reaction as represented in the equation

$$C_mH_nO_k \rightarrow C_xH_yO_z + \text{gas } (H_2, CO, CO_2, CH_4, \ldots.) + \text{coke}$$

Glycerol decomposes when heated in supercritical water at $500^{o}C$ and 340 atm to acetaldehyde, acrolein and gaseous mixture consisting of H_2, CO, CO_2, CH_4, C_2H_4 and C_2H_6. The two possible pathways for the formation of acetaldehyde (C_2) from glycerol (C_3) are initial dehydration and homolytic cleavage of the C-C bond (C-C bond breaks without charge) as shown in the equation (2). Their result supported that the homolytic cleavage of the C-C bond (route 2) is responsible for the formation of acetaldehyde.

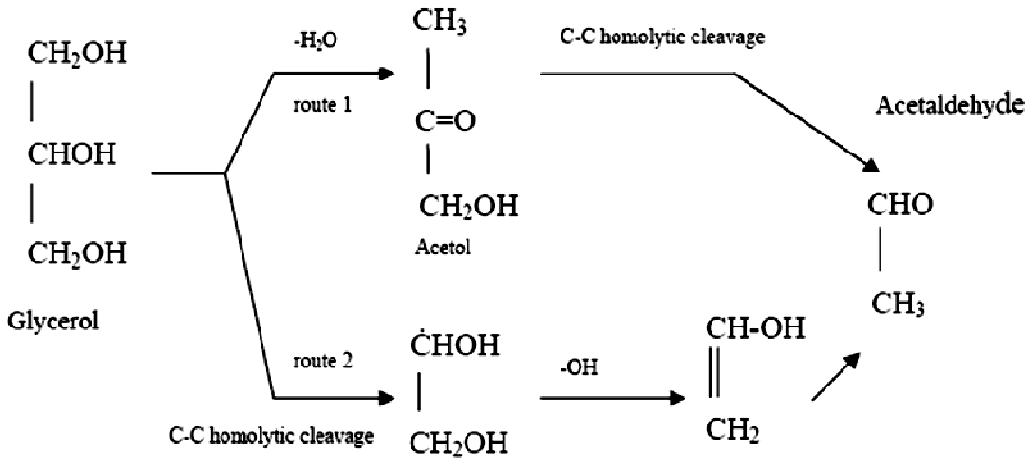

Antal M. J, Mok W.S.L and Roy J. C [31] reported that acrolein could have formed from glycerol via dehydration as shown in the equation

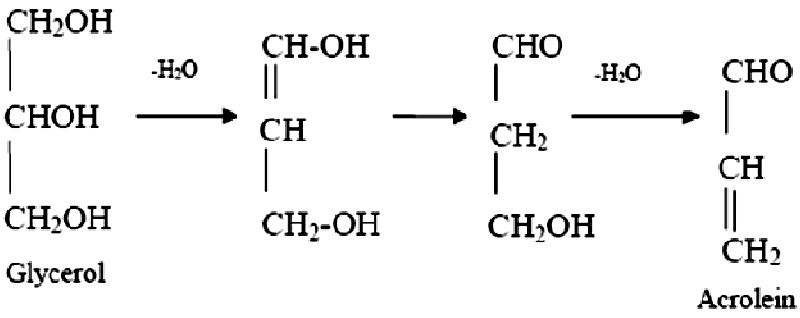

.

The main products from decomposition of glycerol in near and supercritical water were methanol, acetaldehyde, propionaldehyde, acrolein, allyl alcohol, ethanol, formaldehyde, carbon monoxide, carbon dioxide and hydrogen.

Buehler, Dinjus W. E and Kruse A [32] investigated that free radical reaction pathway dominates at lower pressures and/or higher temperatures. The formation of gaseous products is favourable at high temperatures and they follow radical reaction pathway.

It was clear that glycerol, a by-product from production of biodiesel process, has an ability to produce value added products using three possible processes namely pyrolysis, steam gasification and catalytic steam reforming. Results indicated that glycerol pyrolysis

and steam gasification could lead to high quality hydrogen production. Thus, pyrolysis and steam gasification of glycerol processes should be revisited to understand the chemistry of the reactions and process parameters such as temperature, carrier gas flow rate and packing material. In addition, steam to glycerol weight ratio should be tuned to maximise the yield of hydrogen gas.

CHAPTER–3 *EXPERIMENTAL WORK*

In this chapter all the details about the preparation and characterization of samples has been described.

3.1 Methodology

3.1.1 Process

For the synthesis of WC nano particles chemical route was adopted. The experiment designed for it was a refluxing type.

Experiments were performed with the help of condenser and a round bottom flask (1000 ml) which was heated in the temperature range of 250 – 300^0C in a heating mantal. Cold water was circulated with the help of small submersible pump through the condenser to extract the heat out of the condenser which allows the liquid to condense back in the round bottom flask. This process is known as reflux action technique. A guard tube had been applied at the top of the condenser having fused calcium chloride flakes covered with cotton from both sides to avoid the loss of volatile material through the condenser. Experiments were performed for several hours to several days to get the end product. Experimental set up used in present study is shown in fig 3.1 and 3.2 from two different angles.

In order to perform the experiment WO_3, Mg turnings and glycerol liquid was taken in round bottom flask. The condenser assembly was fixed properly. The entire set up was put on heating mantal. Slow heating was done to start the reaction. During heating the vapors of glycerol get condensed and reaction proceeds. As the reaction proceeds the colour of the liquid was monitored. Since WC is a dark coloured substance, so it is expected that variation in colour may occur. Fig 3.3 shows the line diagram of set up and fig 3.4 shows the flow chart for carrying out the experiment.

Fig: 3.1 Set up from one side

Fig: 3.2 Set up from other side

The overall chemical reaction could be formulated as follows:

$$2WO_3 + 2C_3H_8O_3 + 2Mg \longrightarrow 2WC + C + 6MgO + 3CO_2 + 8H_2 \quad (1)$$

$$2WO_3 + 2C_3H_8O_3 + 2Mg \longrightarrow W_2C + 2MgO + 5CO_2 + 8H_2 \quad (2)$$

During the experiments following substances had been taken in the round bottom flask which are given in Table 3.1. However, the only variation done was the refluxing time which is given in Table 3.2.

Table 3.1: Initial ingredients of the experiments

Precursors	**Weight**
WO_3	3g
Magnesium turnings	3g
Glycerol	100 ml

Table 3.2: Duration of experiments

Experiments	**Fluxing Time (hours)**
Sample S_1	96
Sample S_2	168

(Glycerol had been taken because its boiling point is 290^0C and its a long chain carbon compound)

This experiment was carried out continuously for 96 hrs. Light brown residue in the solvent was obtained in the round bottom flask. After the reaction 100 ml of distilled water was added in the flask. This was sonicated for 2 hours to displace the deposited unreacted carbon on the powder. The residue was filtered on whatman filter paper no. 44 Then washing of this residue was carried out with distilled water. Filtrate was then dried in the vacuum oven for 24 hrs. After getting sample in powder, it was subjected to XRD analysis for phase determination. After XRD test acid leaching in the ratio 1:3 was carried out in order to

remove the unwanted phases in the sample. It was observed that with time the colour of liquid becomes dark.

The XRD analysis revealed that that large amount of carbon, unreacted WO_3, MgO phases were present along with WC phase. After acid leaching, the dissolved constituents gets removed to confirm the phases and size of powder. Finally the sample had been subjected to TEM analysis.

In this experimental work two sets of experiments was performed with above contents of constituents required. Only variation was done for refluxing time.

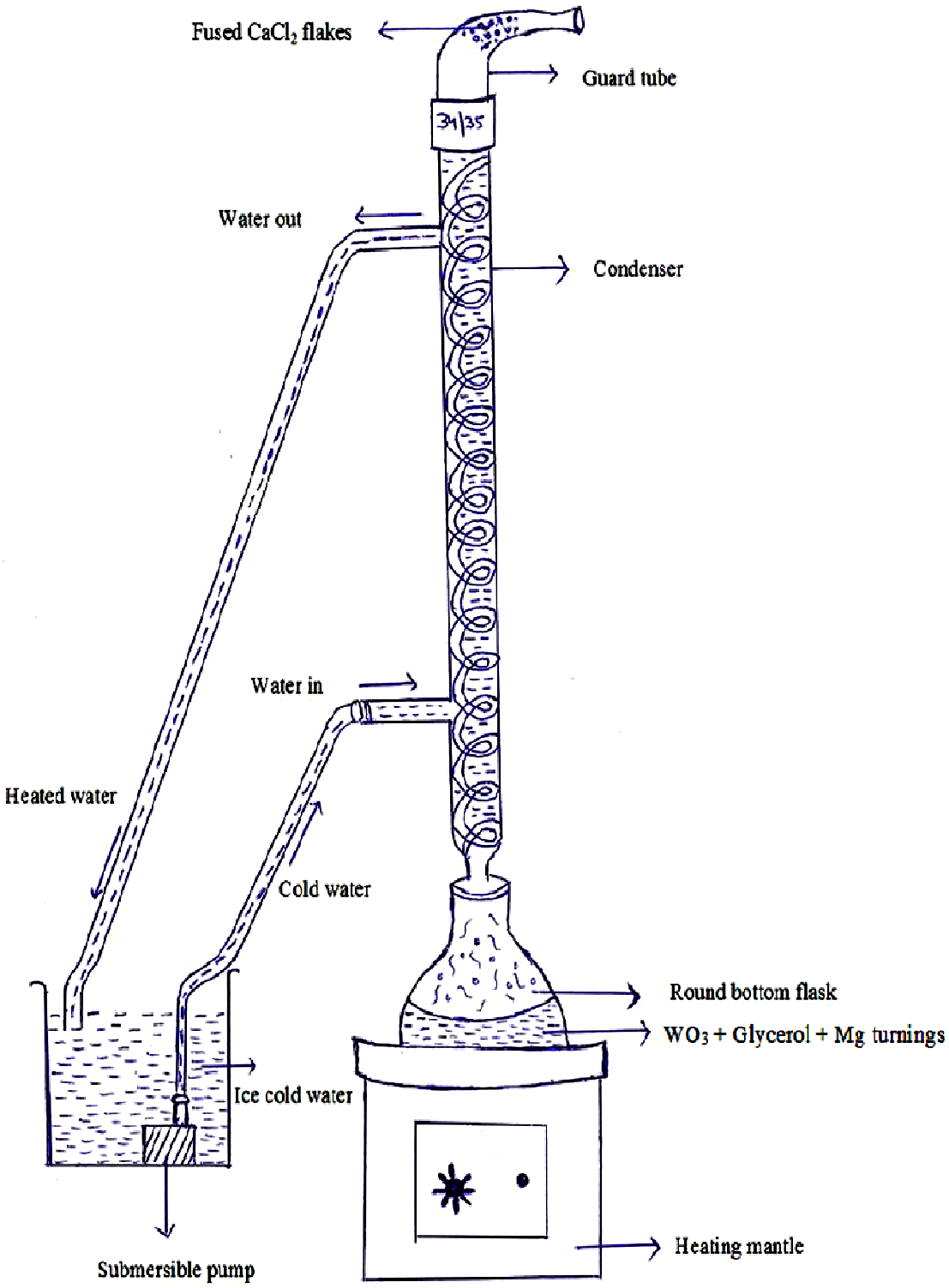

Fig 3.3: Ray diagram of refluxing set up

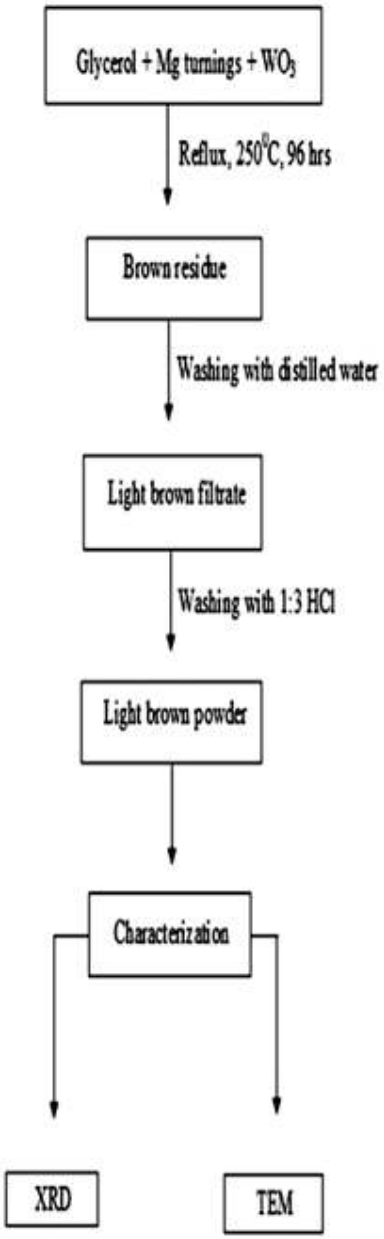

Fig 3.4: Flow chart showing the synthesis route of WC nano particle

3.2 Characterization Techniques

The characterization of tungsten carbide nanoparticles synthesized by simple reductive reaction method was carried out with various characterization methods which are described below:

3.2.1 X-Ray Diffraction Studies (XRD)

X-ray diffraction is the most wide spread technique for determining the phase identification, crystal structure, lattice parameter of the crystalline solids. A typical powder XRD instrumentation consist of four main components such as X-ray source, specimen stage, receiving optics and X-ray detector as shown in fig. The source and detector with its associated optics lie on the circumference of focusing circle and the sample stage at the centre of the circle. The angle between the plane of the specimen and the X-ray source is θ, known as Bragg's angle and the angle between the projection of X-ray and the detector is 2θ. For the XRD analysis, fine powder samples were mounted on the sample holder and the powder was assumed to consist of randomly oriented crystallites. When a beam of X-ray is incident on the sample, X-rays are scattered by each atom in the sample. If the scattered beams are in phase, these interfere constructively and one gets the intensity maximum at that particular angle. The atomic planes from where the X-rays are scattered are referred to as 'reflecting planes'.

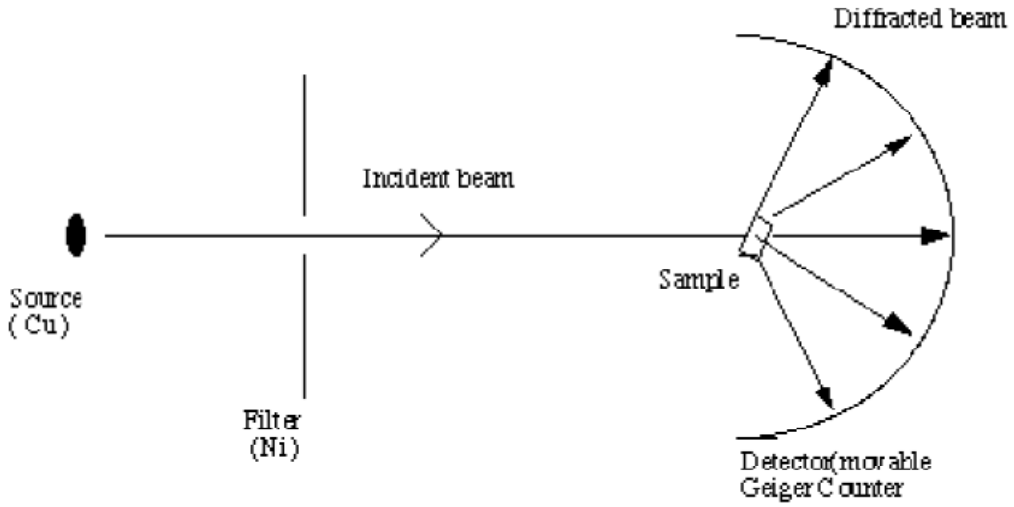

Fig 3.5: X-ray Scattering

The Bragg's law relates the wavelength (λ) of the X-ray reflected the spacing between the atomic planes (d) and the angle of diffraction (θ) as follows:

$$2d \sin \theta = n\lambda .$$

For the first order diffraction, n=1, and knowing θ and λ, one can calculate the interplanar spacing d–value for a particular plane. After recording the X-ray diffraction pattern, first step involves the indexing of XRD peaks. The indexing means assigning the correct Miller indices to each peak of the diffraction pattern. The correct indexing is done only when all the peaks in the diffraction pattern are accounted for the process. There are three main methods for indexing a diffraction pattern,

(i) Comparing the measured XRD pattern with the standard data base (JCPDS cards)
(ii) Analytical methods
(iii) Graphical methods.

In case of fine particles, with reduction in the size of the particles, the XRD lines get broadened, which indicates clearly that particle size has been reduced. Information of the particle size is obtained from the full width at half maximum (FWHMs) of the diffraction peaks. The FWHMs (β) can be expressed as a linear combination of the contributions from the strain (ε) and particle size (L) through the following relation:

$$\mathbf{\cos \theta/\lambda = 1/L + \varepsilon \sin \theta/\lambda}$$

3.2.2 Transmission electron microscope

Transmission electron microscopy (TEM) is used to obtain information from samples that are thin enough to transmit electron. In TEM, the whole area of observation is illuminated using an electron source of adequate intensity. The transmitted electrons are generally used to form either an image or a diffraction pattern of the specimen .The formation of image and electron diffraction in TEM can be understood from schematic ray diagram as shown in fig.3.2 When a crystal of lattice spacing 'd' is illuminated with electrons of wavelength 'λ', the diffracted waves will be produced at specific angles 2θ for n =1, satisfying the Bragg's condition 2d sinθ = nλ. The diffracted waves form diffraction spots on

the back focal plane. In an electron microscope, the use of electron lenses allows the regular arrangement of diffraction spots to be projected on a screen and the electron diffraction pattern can be observed. If the transmitted and the diffracted beam interfere on the image plane, a magnified image can be observed. The space where the diffraction pattern forms is called the reciprocal space, while the space at the image plane or at a specimen is called the real space.

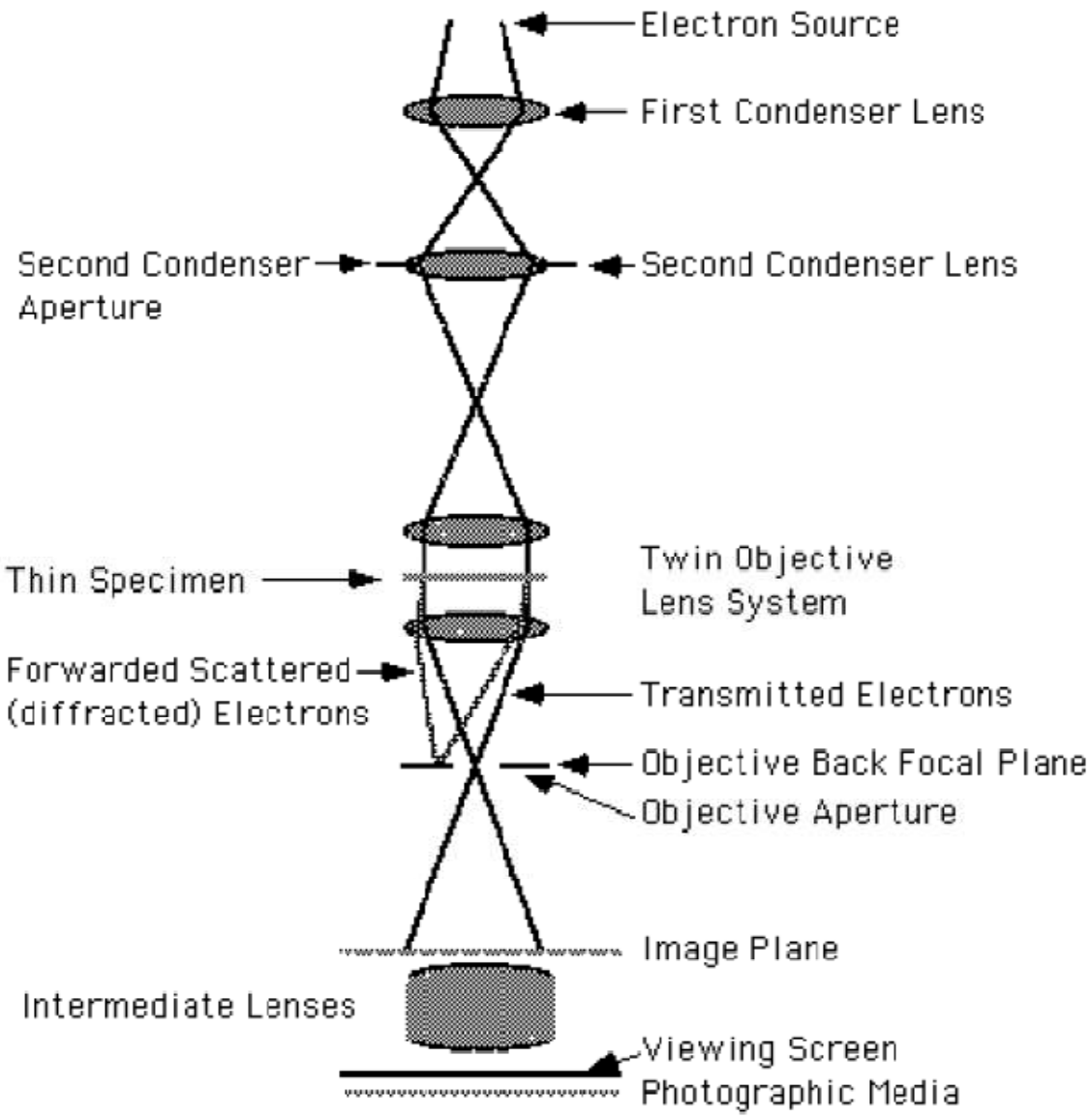

Fig 3.6: Schematic ray diagram of TEM

In TEM, by adjusting the electron lenses, both the microscope images and diffraction patterns can be observed. Thus in the analysis of microstructures of materials, both observation modes can be successfully combined. In an investigation of electron diffraction pattern, the electron microscope images of the nano phosphor is first observed of the whole area and then by inserting an aperture in a specific area and adjusting the electron lenses a diffraction pattern of the area is obtained. The latter observation mode is called selected area electron diffraction (SAED). Because a selected area diffraction pattern can be obtained from each grain, the crystal structure and mutual crystal orientation relationship between adjacent grains can easily be clarified. The observational dimension selected from the object is usually limited to about 0.1 micrometer in diameter. However, in micro diffraction method, the diffraction pattern can be obtained from an area correspondingly to only a few nanometers in diameter. Then, by passing the transmitted beam or one of the diffracted beams through an aperture and changing to the imaging mode, the image with enhanced contrast can be observed. The observation mode using the transmitted beam is called the bright field method, and the image observed is a bright field image. When one of the diffracted beams is selected the observation mode is called as dark field method, and the image observed is a dark field image.

3.2.3 Scanning electron microscope

The scanning electron microscope (SEM) is a type of electron microscope that images the sample surface by scanning it with a high-energy beam of electrons in a raster scan pattern. The electrons interact with the atoms that make up the sample producing signals that contain information about the sample's surface topography, composition and other properties such as electrical conductivity.

The types of signals produced by an SEM include secondary electrons, back scattered electrons (BSE), characteristic x-rays, light (cathodoluminescence), specimen current and transmitted electrons. These types of signal all require specialized detectors that are not usually all present on a single machine. The signals result from interactions of the electron beam with atoms at or near the surface of the sample. In the most common or standard detection mode, secondary electron imaging or SEI, the SEM can produce very high-resolution images of a sample surface, revealing details about 1 to 5 nm in size. Due to the way these images are created, SEM micrographs have a very large depth of field yielding a characteristic three-dimensional appearance useful for understanding the surface structure of

a sample. This is exemplified by the micrograph of pollen shown to the right. A wide range of magnifications is possible, from about X 25 (about equivalent to that of a powerful hand-lens) to about X 250,000, about 250 times the magnification limit of the best light microscopes. Back-scattered electrons (BSE) are beam electrons that are reflected from the sample by elastic scattering. BSE are often used in analytical SEM along with the spectra made from the characteristic X-rays. Because the intensity of the BSE signal is strongly related to the atomic number (Z) of the specimen, BSE images can provide information about the distribution of different elements in the sample. For the same reason, BSE imaging can image colloidal gold immuno-labels of 5 or 10 nm diameter which would otherwise be difficult or impossible to detect in secondary electron images in biological specimens. Characteristic X-rays are emitted when the electron beam removes an inner shell electron from the sample, causing a higher energy electron to fill the shell and release energy. These characteristic x-rays are used to identify the composition and measure the abundance of elements in the sample.

In a typical SEM, an electron beam is thermionically emitted from an electron gun fitted with a tungsten filament cathode. Tungsten is normally used in thermionic electron guns because it has the highest melting point and lowest vapor pressure of all metals, thereby allowing it to be heated for electron emission, and because of its low cost. Other types of electron emitters include lanthanum hexaboride (LaB_6) cathodes, which can be used in a standard tungsten filament SEM if the vacuum system is upgraded and field emission guns (FEG), which may be of the cold-cathode type using tungsten single crystal emitters or the thermally-assisted Schottky type, using emitters of zirconium oxide.

The electron beam, which typically has an energy ranging from a few hundred eV to 40 keV, is focused by one or two condenser lenses to a spot about 0.4 nm to 5 nm in diameter. The beam passes through pairs of scanning coils or pairs of deflector plates in the electron column, typically in the final lens, which deflect the beam in the *x* and *y* axes so that it scans in a raster fashion over a rectangular area of the sample surface.

When the primary electron beam interacts with the sample, the electrons lose energy by repeated random scattering and absorption within a teardrop-shaped volume of the specimen known as the interaction volume, which extends from less than 100 nm to around 5 μm into the surface. The size of the interaction volume depends on the electron's landing

energy, the atomic number of the specimen and the specimen's density. The energy exchange between the electron beam and the sample results in the reflection of high-energy electrons by elastic scattering, emission of secondary electrons by inelastic scattering and the emission of electromagnetic radiation, each of which can be detected by specialized detectors. The beam current absorbed by the specimen can also be detected and used to create images of the distribution of specimen current. Electronic amplifiers of various types are used to amplify the signals which are displayed as variations in brightness on a cathode ray tube. The raster scanning of the CRT display is synchronised with that of the beam on the specimen in the microscope, and the resulting image is therefore a distribution map of the intensity of the signal being emitted from the scanned area of the specimen. The image may be captured by photography from a high resolution cathode ray tube, but in modern machines is digitally captured and displayed on a computer monitor and saved to a computer's hard disc.

Magnification in a SEM can be controlled over a range of up to 6 orders of magnitude from about X 25 to X 250,000 and exceptionally to 2 million times in the Hitachi S-5500 in-lens Field Emission SEM, imaging a specimen area about 60nm wide with resolution up to 0.4 nm. Unlike optical and transmission electron microscopes, image magnification in the SEM is not a function of the power of the objective lens. SEMs may have condenser and objective lenses, but their function is to focus the beam to a spot, and not to image the specimen. Provided the electron gun can generate a beam with sufficiently small diameter, an SEM could in principle work entirely without condenser or objective lenses, although it might not be very versatile or achieve very high resolution.

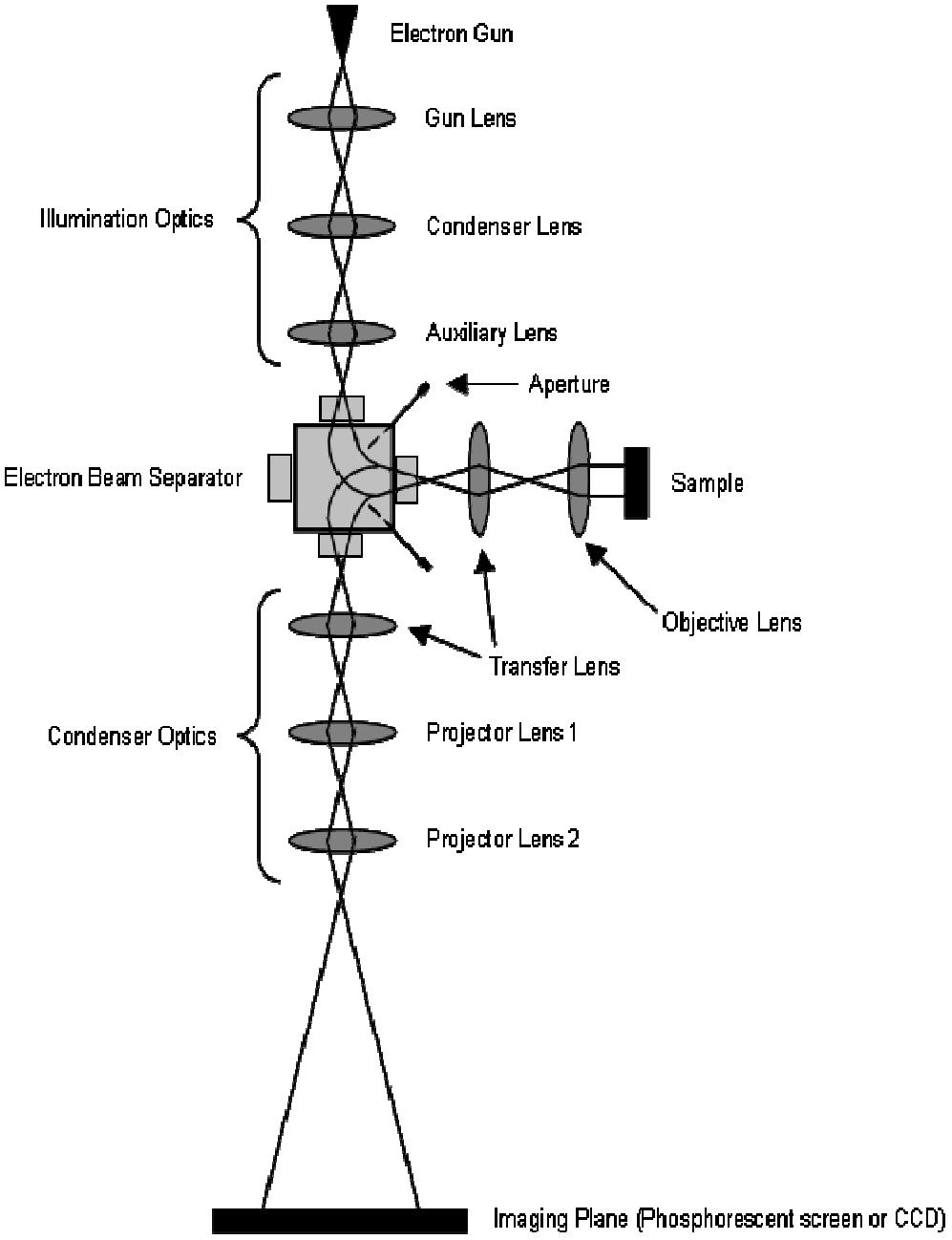

Fig 3.7: Schematic ray diagram of SEM

Refluxing is the technique used in chemistry to supply/apply energy to reaction over an extended period of time. In this process the vapours condenses and return to condensate to the system from which it has originated.

Possible reaction that may occur during refluxing of glycerol ($C_3H_8O_3$) with WO_3 at a temperature of 290^0C can be written as

$$2WO_3 + 2C_3H_8O_3 + 2Mg \longrightarrow 2WC + C + 6MgO + 3CO_2 + 8H_2 \quad (1)$$

$$2WO_3 + 2C_3H_8O_3 + 2Mg \longrightarrow W_2C + 2MgO + 5CO_2 + 8H_2 \quad (2)$$

4.1 X-Ray diffraction analysis

The samples S_1 and S_2 were characterized by X-ray powder diffraction (XRD) with Cu (Kα) radiation (λ = 1.5443A˚). The X-ray diffractogram of sample S_1 in the as prerared condition showed the presence of WC, W_2C, WO_3 and MgO phases as shown in Fig 4.1. However , after acid leaching the MgO was removed which is shown in fig 4.2.

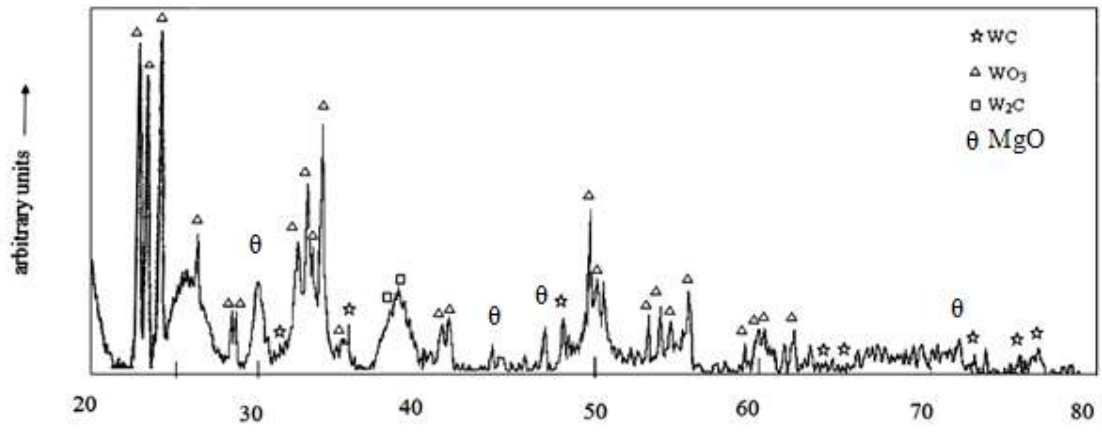

Fig 4.1: XRD of sample S_1

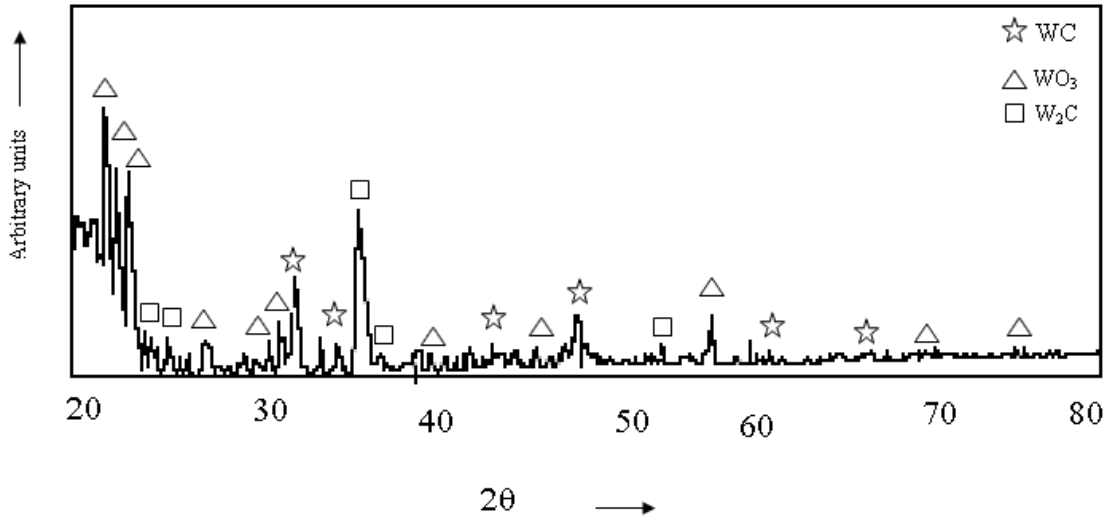

Fig 4.2: XRD of 1:3 acid leached sample S_1

Fig 4.3 is X-ray diffractogram of sample S_2. Here in this case the volume fraction of WC is observed to increase. Fig 4.4 shows the X-RAY diffractogram of leached sample S_2 which present the similar view as in case of fig 4.3.

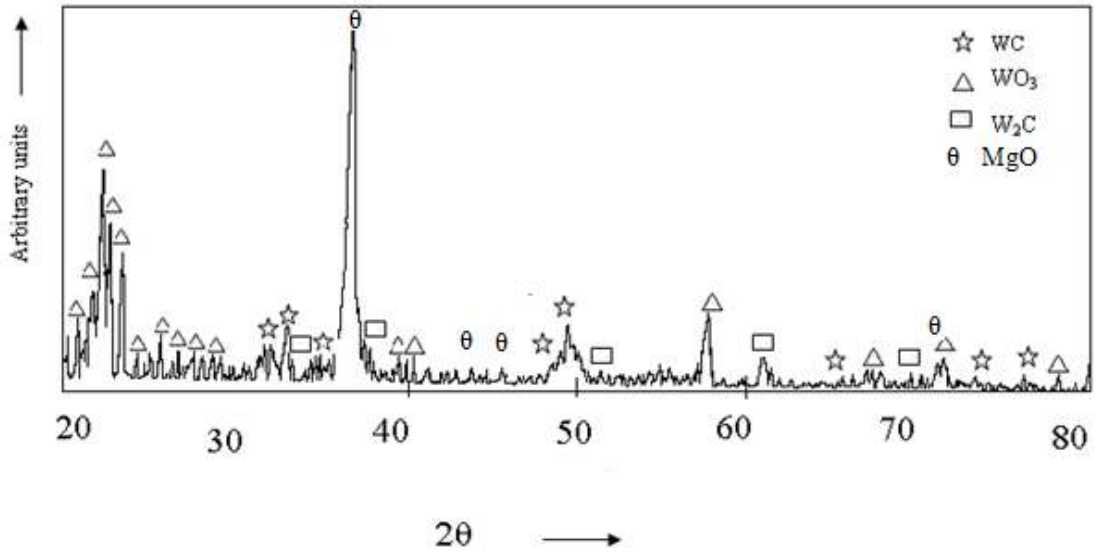

Fig 4.3: XRD of sample S_2

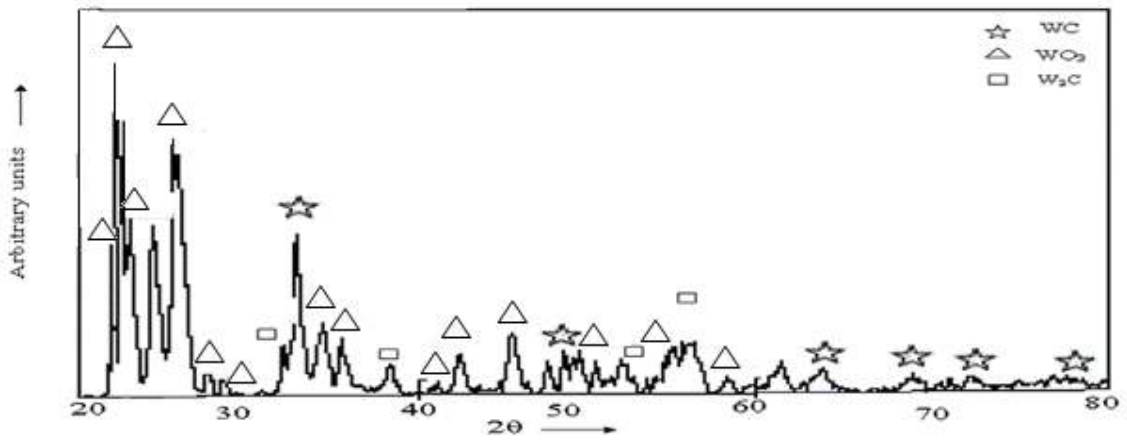

Fig 4.4: XRD of 1:3 acid leached sample S_2

Since in our X-ray diffractogram WC, W_2C, MgO and unreacted WO_3 was observed, so the above proposed reaction is one of the possibility to occur. However, during refluxing action formation of complex compound may also occur.

The detailed XRD analysis shows that with the increase in reaction time from 96 hours to 168 hours the peak intensities of WC increases which shows that volume fraction of WC phase has increased. The particle size calculated from peak broadening also shows that the size of particle has also reduced.

The degree of orientation of different planes is not similar. In order to investigate a possibility of the preferred orientation, a comparison of peak intensity with standard specimen was done using Harris analysis. Mathematical expression using Harris analysis is given below:

$$P(h_i k_i l_i) = \frac{I(h_i k_i l_i)}{I_0(h_i k_i l_i)} \left[\frac{1}{n} \sum_{i=1}^{n} \frac{I(h_i k_i l_i)}{I_0(h_i k_i l_i)} \right]^{-1}$$

where P(hkl) is texture coefficient of the plane specified by Miller Indices (hkl), I(hkl) and I_o(hkl) are the specimen and standard intensities respectively for a given peak and n is the number of diffraction peaks. The calculated texture coefficients of all the phases are tabulated in table 4.1 and 4.2. Plane (100) is highly textured in when the reaction time is 96 hours. When the reaction time is increased to 168 hours the texture coefficient is increased to 1.43.

Table 4.1: Calculations of texture coefficient of nano powders (sample S_1)

Phase in Sample 1	Crystal structure	Particle Size (XRD) nm	JCPDS CARD No.	Planes	Texture Coefficient
WC	Hexagonal	160	25-1047	100	1.03
				101	0.81
				001	0.74
WO_3	Triclinic	330	83-0949	002	0.72
				020	1.14
				200	0.75
W_2C	Hexagonal	80	20-1315	101	0.73
				100	1.05

Table 4.2 : Calculation of texture coefficient of nano powders (sample S_2)

Phase in Sample 2	Crystal structure	Particle Size (XRD) nm	JCPDS CARD No.	Planes	Texture Coefficient
WC	Hexagonal	120	25-1047	100	1.43
				101	0.84
				001	0.68
WO_3	Triclinic	270	83-0949	002	0.72
				020	1.01
				200	0.87
W_2C	Hexagonal	70	20-1315	101	0.83
				100	1.01

4.2 Transmission electron microscopy results

Transmission Electron Microscope results of the synthesized particles were done to know the particle size of synthesized powder. From the selected area diffraction pattern the lattice constant of different phases can be determined. For TEM study the powders were suspended in ethanol. One drop of this suspension was dropped on carbon coated copper grid. The ethanol was allowed to evaporate leaving powders on grid. The sample was analysed under TEM. Fig 4.5 and 4.6 shows the micrograph of synthesised powder taken from

different areas. Looking at the features of micrograph it can be said that there are different types of phases which varies from spherical to elliptical, cylindrical to rectangular as can be seen in fig 4.5 and 4.6. In these micrographs a powder having faceted structure is of WC and elongated needle type of faceted structure is of W_2C.

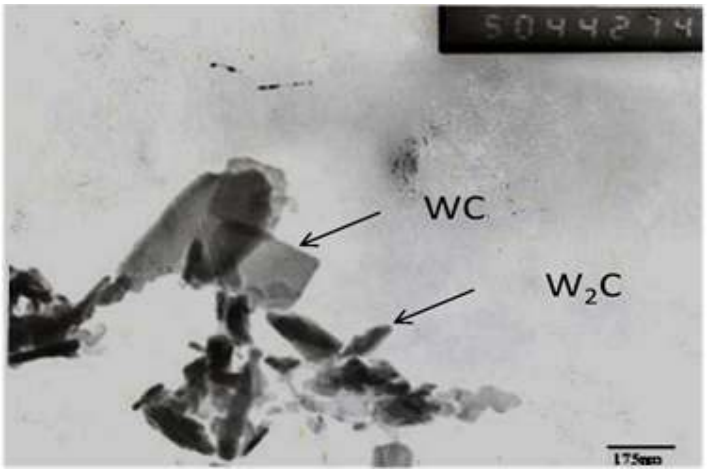

Fig 4.5: TEM image of sample S_1

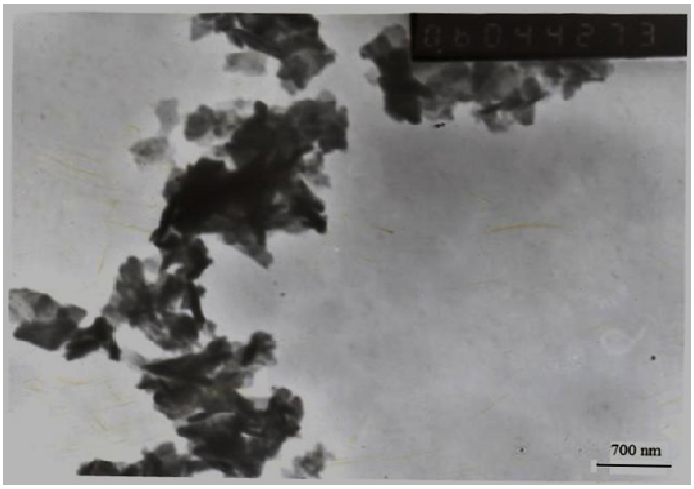

Fig 4.6: TEM image of sample S_1 taken from other portion

The overall structure gives complex type of phenomenon from which it can be concluded that reduction of WO_3 with glycerol is feasible but condition has to be optimized. It is essential to optimize the role of reducing element magnesium and also the condition required for reduction by using different reducing agents.

Selected area electron diffraction (SAED) is also shown in the fig 4.5 which has confirmed that [101] and [110] planes of WC, [200] and [002] planes of W_2C and [032] and [242] planes of WO_3 that exists in the system.

Fig 4.7: SAED pattern of WC particle of sample S_1

The X-ray analysis and TEM studies indicated that the particles which are synthesized are within the nanosize range. However, a detail analysis will reveal phases present in it.

4.3 Scanning electron microscopy results

Fig 4.6 (a, b, c, d) shows the SEM micrograph of powder (sample S_1) synthesized during reflux reaction of 96 hours and leached. The structural feature shows the agglomerated particle of nanosize. The presence of rod like structure along with faceted morphology is an indicative of the presence of WC or W_2C phases in the system. However, the round shape powders may be of carbon which are in the unreacted form.

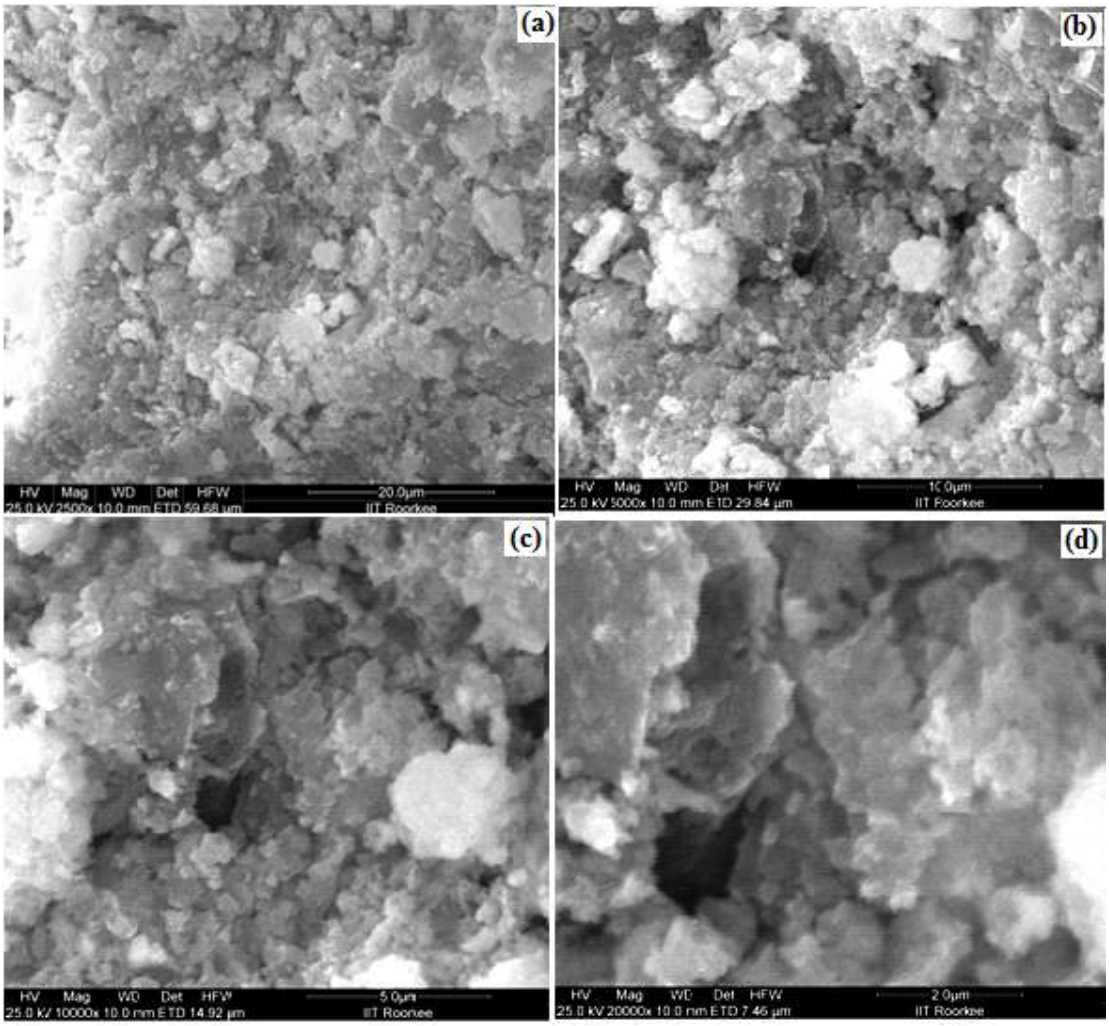

Fig 4.8: SEM image of Sample S_1

Fig 4.7 (a, b, c, d) shows SEM micrograph of sample S_2 during reflux reaction of 168 hours. Here also fine size powders can be seen. The structural features are similar but with variation in shape of the synthesized powders.

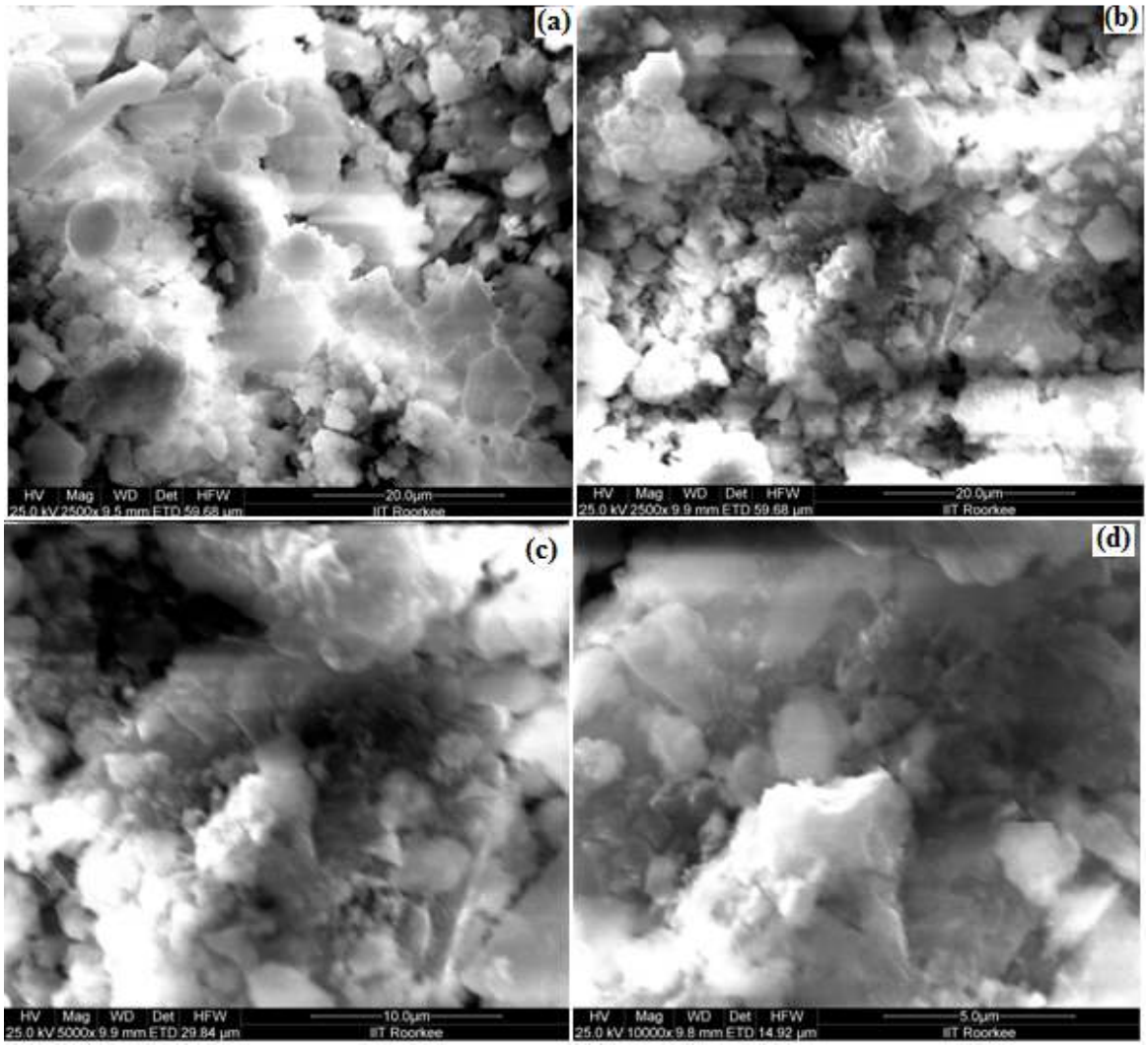

Fig 4.9: SEM image of Sample S_2

4.4 EDAX Results

The EDAX analysis of sample S_1 and sample S_2 is shown in fig 4.8 and 4.9 respectively. It shows the presence of carbon, oxygen and tungsten as major constituents which further confirmed the formation of intermetallic phase WC or W_2C.

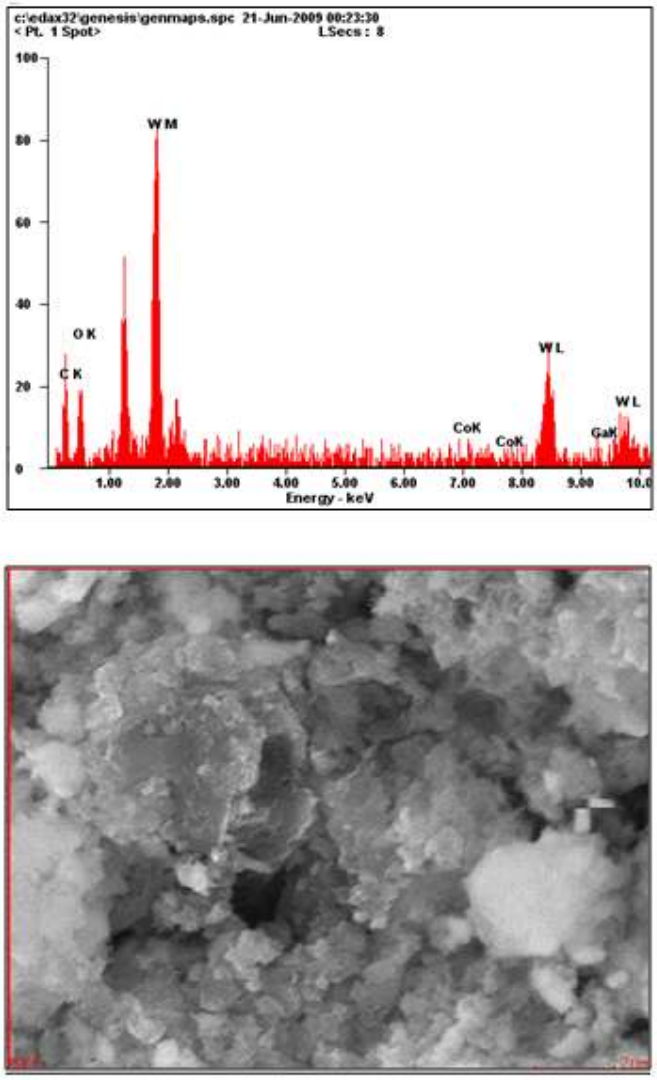

Fig 4.10: EDAX of sample S_1

Table 4.3: Element composition of sample S_1

Element	Wt %	At %
carbon	26.69	62.38
Oxygen	15.55	27.29
Cobalt	01.43	00.68
Tungsten	52.14	07.96
Gallium	04.18	01.69

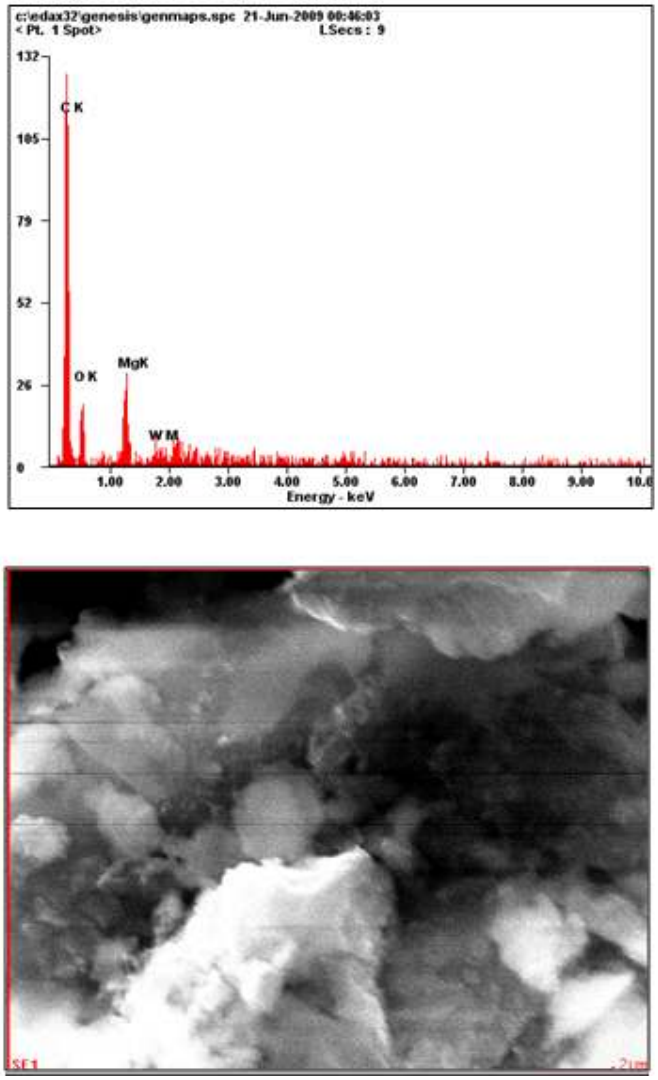

Fig 4.11: EDAX of sample S_2

Table 4.3: Element composition of sample S_2

Element	Wt %	At %
Carbon	72.41	80.78
Oxygen	18.92	15.85
Magnesium	05.74	03.16
Tungsten	02.93	00.21

4.5 Proposed reaction mechanism

TEM studies indicate that reduction of WO_3 takes place by adsorption of carbon at the surface of WO_3 first. These carbon particles engulf the WO_3 particles as shown in Fig 4.6, the variation in contrast observed indicates that the transformation of WO_3 to WC is a multiphase phenomenon. As the concentration of carbon increases at the surface, WO_3 particles bind itself within the carbon layer. In a report Swift and Koc [29] have reported the formation of WC from carbon coated WO_3 precursors. As the concentration of carbon increases on the surface of WO_3 the process of transformation of WO_3 to WC starts as is evident from the faceted morphological feature.

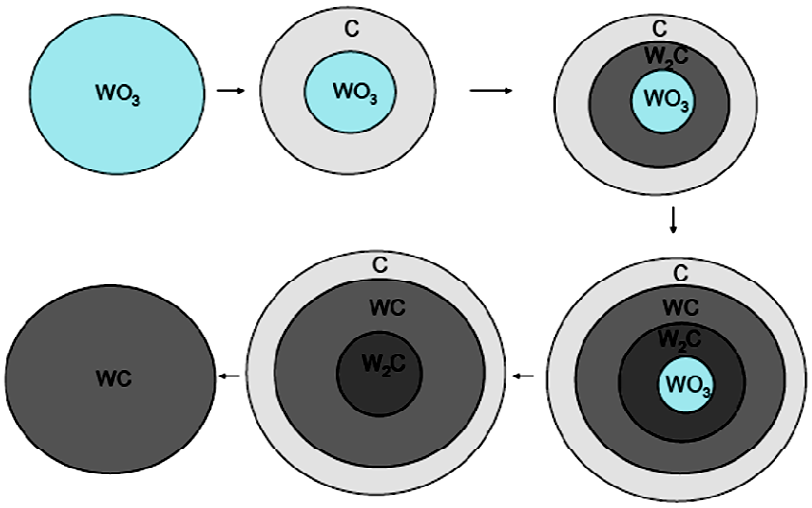

Fig 4.12: Proposed reaction mechanism

The presence of amorphous carbon on the outer surface facilitates the process of reduction of WO_3 to WC [28]. However, because of conductive atmosphere and also the formation of ethane and hydrogen during the course of reaction leads to the formation of such features.

For the formation of WC powder, it is estimated that some reducing agent along with carbon source should be present. Since Mg act as reducing element so it is essential to have free carbon on the surface of WO_3. This is only feasible if glycerol undergoes thermal cracking. This type of reaction is not feasible in reflux action. However, the possible mechanism may lead to decomposition of glycerol and formation of gaseous products.

Chapter-5 *CONCLUSIONS AND FUTURE SCOPE*

In this study, it has been observed that thermo chemical route (refluxing method) is one of the suitable techniques for the synthesis of WC nano particles. Since the process is low temperature synthesis (250-300^{0}C) as compared to the other routes which has been followed for synthesis of WC nano particles, it makes the process more versatile.
From the present work, the following conclusions have been drawn:

1. It is possible to synthesize WC nano particles using reflux action technique by different organic compounds having double and triple bonds to react readily with WO_3.
2. During synthesis several other phases has also formed which include W_2C, unreacted carbon and unreacted Mg compound.
3. It is possible to leach out other phases except carbon.
4. The phases which are present in synthesised powder show the possibility to synthesize WC nano particles of the suitable variation in process parameters.

Considering all aspects it is suggested that a systematic study to establish a mechanism of formation of WC and W_2C should be done to optimise the process. Further reactions would be carried out with other tungsten sources like tungstic acid and tungsten chloride to get the maximum possibility of WC phase through it.

REFERENCES

1. V.K. Sarin, "Cemented Carbide Cutting Tools", Advances in powder Technology. Ed. D. Y. Chin, ASM, 1981, pp. 253-287.
2. E. M. Trent, "Metal Cutting", Butterworth's, Boston, 2nd Ed., 1984.
3. V. K. Sarin, "Cemented Carbide Cutting Tools", Advances in Powder Technology, Ed. D. Y. Chin, ASM, pp. 253-287, 1981.
4. "Tungsten", McGraw-Hill Encyclopaedia of Science and Technology, 7th Ed. 1992.
5. H. Kolaska, "The Dawn of the Hardmetal Age", Powder Metallurgical International, v24, no. 5, p 311-314, 1992.
6. T. B. Massalski (Ed.), "Binary Alloy Phase Diagrams", Vol. 1: Alloys; Vol. 2: Phase Diagrams. ASM Int., Materials Park, Ohio, 1990.
7. R. Telle, "Boride and Carbide Ceramics", in Structure and Properties of Ceramics", Vol. 11, Ed. M. V. Swain, VCH, New York, 1994.
8. V. H.Hartmann, F. Ebert, O. Bretschneider, Z. Anorg.Allg. Chem., (1931) 198, 116.
9. E. A Brandles , "Smithels Metal Reference Book", 6th Ed. Butterworth's, Boston, 1983.
10. K. Scherer, US Patent 1,549,615 (application Oct. 31, 1923; patented 1925).
11. P. Schwarzkopf, Deutsche Edelstahlwerke, AG German Patent 720,502 (patented 1929, issued 1942).
12. A. E. McHale, "Phase Equilibria Diagrams – Phase Diagrams for Ceramists", Vol. 10, Fig. 8969, the American Ceramic Society, Westerville, Ohio, 1994.
13. H. J. Scussel, "Friction and Wear of Cemented Carbides", ASM Handbook, Vol. 18, ASM Int., pp. 795, 1992.
14. R. Dagani, "Nanostructured Materials Promise to Advance Range of Technologies", Chemical & Engineering News, Nov. 23 1992, 18-24.
15. H. J. Scussel, "Friction and Wear of Cemented Carbides", ASM Handbook, Vol. 18, ASM Int., pp. 796, 1992.
16. P. Seegopaul and L. E. McCandlish, "Nanostructured WC-Co Powders: Review of Application, Processing and Characterization Properties", Adv. Powder Metall. Part. Mater 3, 13/3-13/15, 1995.
17. J. J. Stiglich, C. C. Yu and T. S. Sudarshan, "Synthesis of Nano WC/Co for Tools and Dies", Tungsten Refract. Met. 3-1995, Proc. Int. Conf., 3rd 1995 (Pub. 1996), 229-236.

18. N C. Angastiniotis, B.H. Kear, L.E. McCandlish, K.V. Ramanujachary, M. Greenblatt, "Formation and Alloying of Nannostructured β-W Powders", Nanostructured Materials, Vol. 1, (1992) pp. 293-302
19. A. T. Santhanam, P. Tierney, and J. L. Hunt, "Cemented Carbides", Metals Handbook, ASM Int., Vol. 2, 10th Ed. pp. 950-977, 1990.
20. L. Zhang, T. E. Madey, "Initial Stages of Sintering of Nanostructured WC-7wt. %Co", NanoStructured Materials, 2, 487-493, 1993.
21. L.E. McCandlish, B.H. Kear and B.K Kim " Chemical Processing and properties of nanostructured WC-Co Materials(1992) Vol 1, pp. 119-124
22. Y. T.Zhu and A. Manthiram "Influence of Processing Parameters on the Formation of WC- Co Nanocomposite Powder Using a Polymer as Carbon Source". (1996) 407.
23. L.Geo, B.H. Kear "Synthesis of Nanophase WC Powder by a Displacement Reaction Process". Nanostructured Materials, Vol. 9, pp 205-208, 1997
24. Z. G. BAN., L.L Shaw., "Synthesis and Processing of Nanostructured WC-Co Materials". Journal of Material Science, 37 (2002) 3397- 3403
25. J. Michael Hudson, W. John Peckett, and J.F. Peter Harris. "Low – Temperature Sol- Gel Preparation of Ordered Nanoparticles of Tungsten Carbide/ Oxide", Ind. Eng. Chem. Res. 2005, 44, 5575-5578.
26. B.S.Terry and D. C. Azubike, "Reduction- Carburization of Wolframite (FeWO4):Part1-Reduction of Natural Wolframite Concentrate," Trans Inst. Mineral. Metall. (Sect.C: Mineral Process. Extr. Metall.), 99(1990), 167-74.
27. Chunli Guo, Lio Yi, Xiaojian Ma, Yitai Qian, and Liqiang Xu. "Synthesis of Tungsten Carbide nanocrystal via a Simple Reductive Reaction". Chemistry Letters Vol. 35 No. 11 (2006).
28. Akshay Kumar, K. Singh and O. P. Pandey "Reduction of WO_3 to nano WC by thermo chemical reaction route" 2008.
29. G. A. Swift, R. Koc, Journal of material science 35 (2000) 2109.
30. Wang D, D. Montané, E. Chornet, "Catalytic steam reforming of biomass-derived oxygenates: acetic acid and hydroxyacetaldehyde" Applied Catalysis A: General **143,** 245-270 (1996).
31. Antal, M.J., W.S.L. Mok, J.C. Roy and A.T. Raissi, "Pyrolytic sources of hydrocarbons from biomass", Journal of Analytical and Applied Pyrolysis **8,** 291-303 (1985).

32. Buehler, W. E Dinjus, H.J. Ederer, A. Kruse and C. Mas, “Ionic reactions and pyrolysis of glycerol as competing reaction pathways in near- and supercritical water” The Journal of Supercritical Fluids **22,** 37-53 (2002).